Supporting Information

Experiments:

Materials and methods:

Methanol (99.8%, anhydrous), ethanol (99.8%, anhydrous), 1-propanol (99%), 1-butanol (99%), 1-pentanol (99%), benzyl alcohol (99%), toluene (99.5%), $Mg(NO_3)_2 \cdot 4H_2O$(⩾99.0%), $Ni(NO_3)_2 \cdot 6H_2O$ (>99.0%) were purchased from ACROS Organics. $Al(NO_3)_3 \cdot 9H_2O$ (⩾98%), $Cu(NO_3)_2 \cdot 2.5H_2O$ (98%), $Zn(NO_3)_2 \cdot 6H_2O$ (99.0%), $RuCl_3 \cdot H_2O$(99.0%), Na_2CO_3, o-phenylenediamine, 2-nitroaniline, benzimidazole, 3,4-diaminopyridine, 4-methyl-o-phenylenediamine, 4-methoxy-o-phenylenediamine, 3,3'-diaminobenzidine, 4-chloro-o-phenylenediamine, 2,3-diaminopyridine were purchased from Sigma Aldrich. NaOH (98%) was purchased from Merck KGaA company. 2-methyl-6-nitroaniline, 4-(tert-butyl)-o-phenylenediamine, 4,5-dimethyl-2-nitroaniline, 4-methyl-2-nitroaniline, 4-methoxy-2-nitroaniline, 4-chloro-2-nitroaniline were purchased from Alfa Aesar. All chemicals were used as received without further purification.

^{1}H and ^{13}C NMR spectra were recorded on a Varian AMX400 spectrometer. Powder X-ray analysis was performed on a Bruker XRD diffractometer using Cu Kα radiation and the spectra were recorded in the 2θ angle range of 5°-70°. Elemental analyses and leaching experiments were performed on a Perkin Elmer instrument (Optima 7000DV). Mass spectra were recorded on LTQ Orbitrap XL (ESI+). Kinetic modeling of the 2-nitroaniline conversion to the main products benzimidazole and N-methylbenzimidazole was performed with DynaFit 4.[1]

Catalyst characterization

XRD characterization of the different catalysts before (figure s1, a) and after calcination (figure s1, b) was performed. Hydrotalcite-like precursors (Figure s1, a) exhibit sharp and symmetrical reflections at 11.71, 23.21, 60.61 and 61.81 (ascribed to the diffraction by the (003), (006), (110) and (113) planes) and broad and asymmetric reflections at 34.71, 38.81 and 46.01 (ascribed to the diffraction by the (102), (105) and (108) planes), according to reported data[2]. After calcination at 460 °C, the double-layered structure is converted into that of a mixed-oxide composition, where a residual Mg(Al)O phase is visible while no CuO oxide phase is shown, indicating an homogeneous dispersion of the active metal[3].

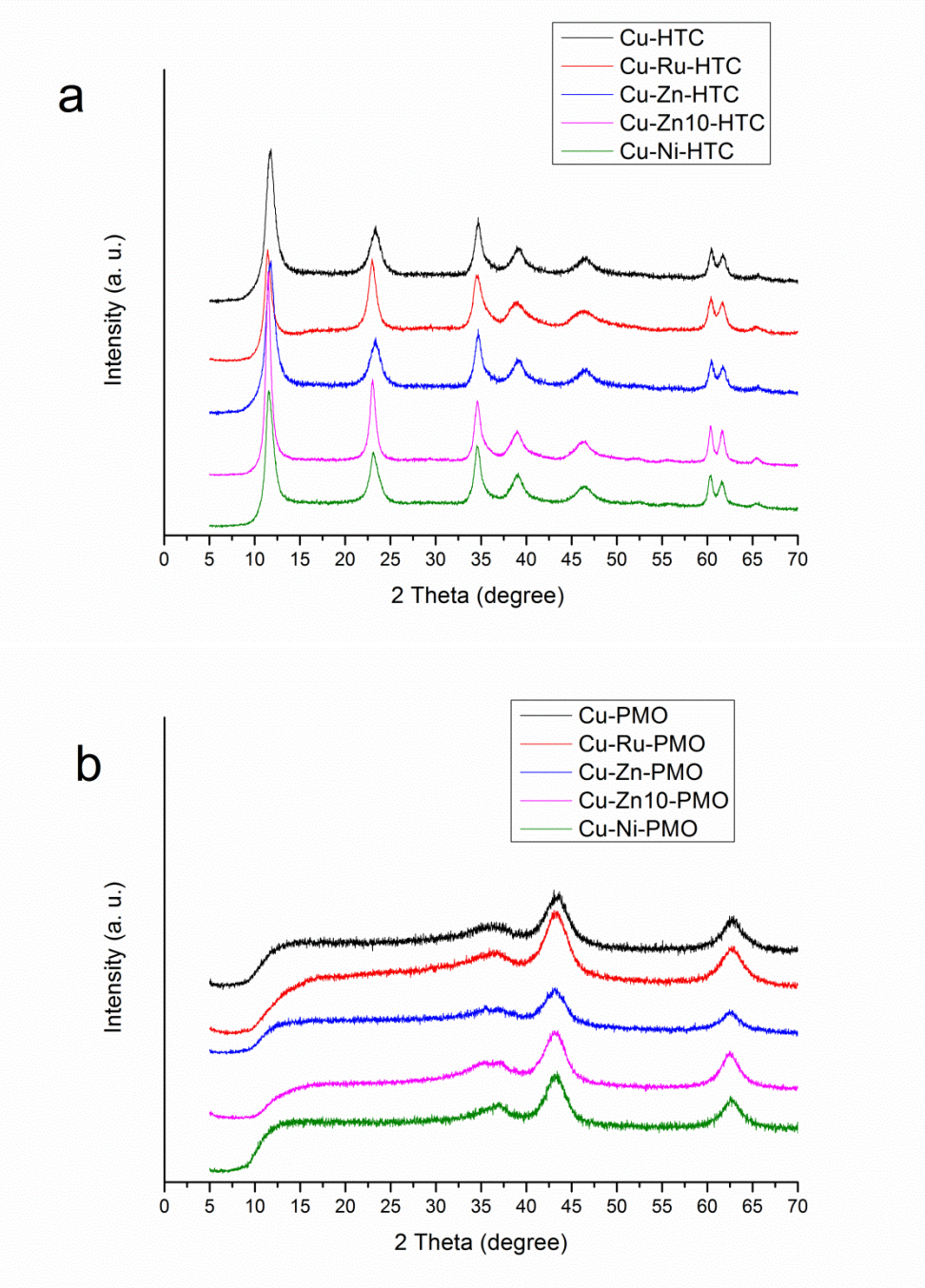

Figure S1. XRD patterns of the synthesized hydrotalcites (a) and the corresponding porous metal oxides (PMOs) after calcination (b).

Table S1. Elemental composition of Cu-M-PMO catalysts determined by ICP analysis.

Cat.	Al (wt.%)	Cu (wt.%)	Mg (wt.%)	M (wt.%)
Cu-PMO	12.2	17.4	22.2	
Cu-Zn-PMO	9.2	16.5	21.8	5.8
Cu-Zn_{10}-PMO	11.4	16.6	21.7	6.5
Cu-Ni-PMO	8.9	16.2	21.1	5.0
Cu-Ru-PMO	9.8	14.1	20.7	0.6

Table S2. Product distribution in the benzimidazole synthesis from 1,2-benzenediamine at different substrate loading and constant catalyst amount.[a]

Entry	Substrate (mmol)	Conversion (%)[b]	Selectivity %[b]		
			1a (%)	**1b** (%)	**1c** (%)
1	0.6	100	58	42	0
2	0.8	95	53	40	2
3	1.0	79	46	27	6
4	1.5	69	33	23	13
5	2.0	53	27	14	13

a. Reaction conditions: Cu-PMO (50mg), methanol (3ml), 250 °C, 3h. b. Determined by GC analysis.

Table S3. ICP of the liquid samples after reaction with Cu-PMO and Cu-Zn-PMO catalysts.[a]

Catalyst	Cu (mg/L)	Mg (mg/L)	Al (mg/L)	Zn (mg/L)
Cu-PMO	<1	15	11	-
Cu-Zn-PMO	<1	6	1	3

a. Reaction conditions: Catalyst (50 mg), 1,2-benzenediamine (1 mmol), methanol (3ml), 250 °C, 3h.

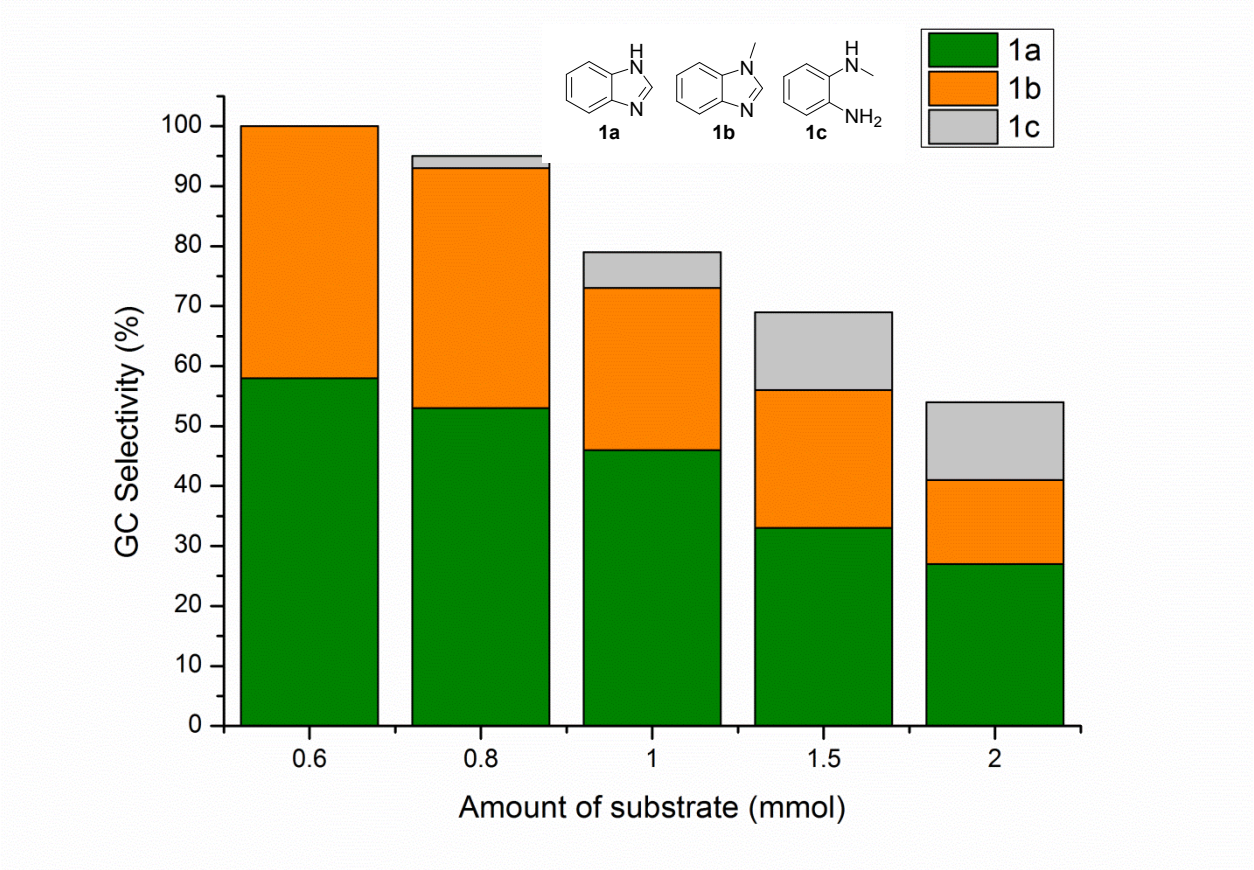

Figure S2. GC selectivities of **1a**, **1b** and **1c** at different substrate to catalyst ratios (the remainder is the unconverted 1,2-diaminobenzene). Reaction conditions: substrate (amount indicated in the bar chart), Cu-PMO (50mg), methanol (3ml), 250^{o}C, 3h.

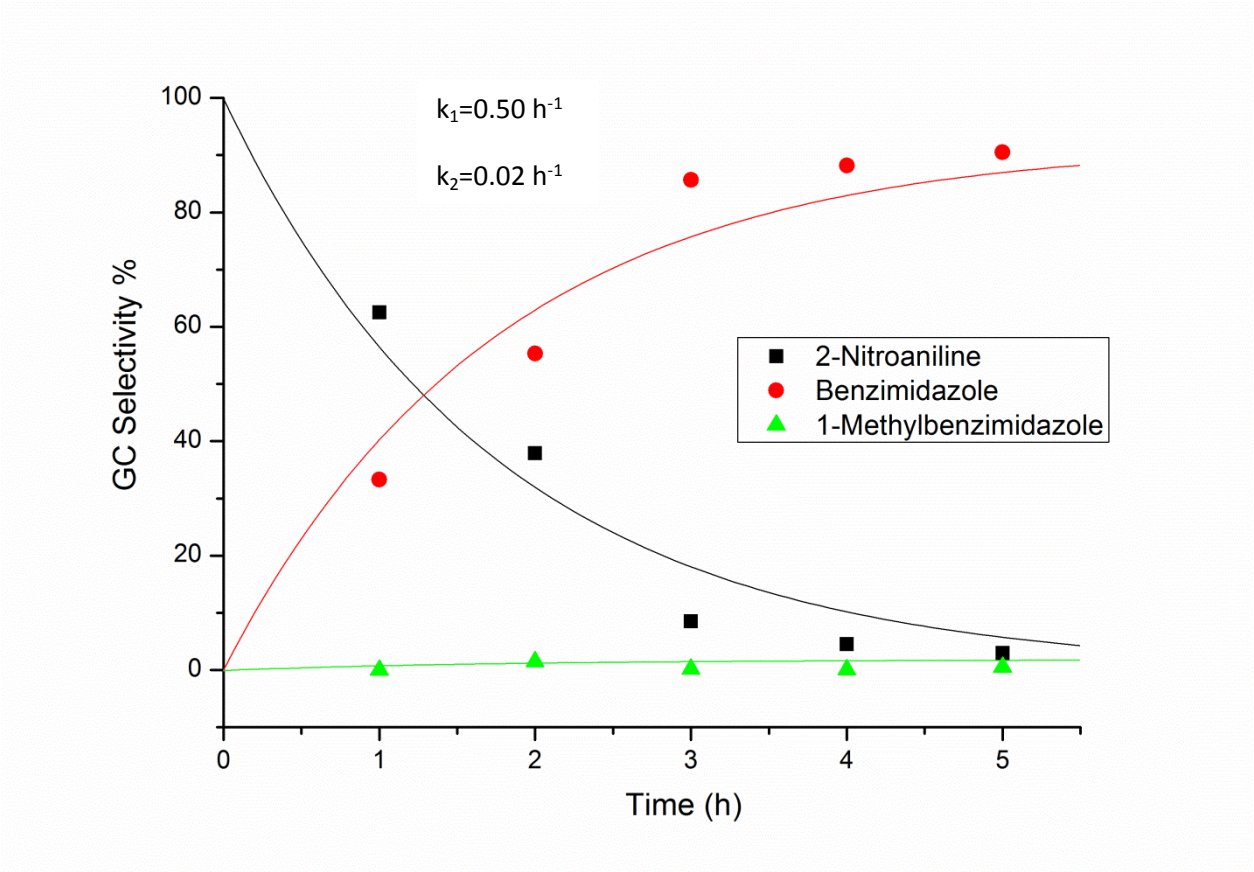

Figure S3. Kinetic profile for the 2-nitroaniline conversion to benzimidazole and 1-methylbenzimidazole. K_1 and k_2 values refer to the reaction rate constants for the formation of benzimidazole and 1-methylbenzimidazole, respectively. Reaction conditions: Cu-Zn-PMO (50 mg), 2-nitroaniline (1 mmol), methanol (3 ml), 250 ^{o}C.

Characterization of new benzimidazole compounds

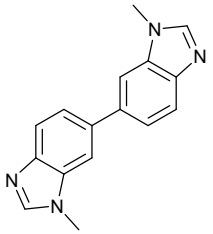

3,3'-dimethyl-3*H*,3'*H*-5,5'-bibenzo[*d*]imidazole

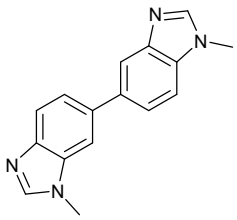

1,3'-dimethyl-1*H*,3'*H*-5,5'-bibenzo[*d*]imidazole

Light yellow oil (yield: 15%). ^{1}H-NMR (400 MHz, DMSO-d6): δ 8.21, 8.18 (d, Ar-H), δ 8.00 (s, Ar-H), δ 7.91, 7.89 (d, Ar-H), δ 7.73-7.55 (m, Ar-H), δ 3.91, 3.87 (d, CH_3) ppm; ^{13}C NMR (101 MHz, DMSO-d6) δ 145.69, 145.59, 145.43, 144.53, 136.22, 135.76, 135.61, 135.41, 122.47, 121.67, 121.57, 119.84, 117.97, 117.86, 110.86, 108.95, 31.22, 31.20 ppm. HMRS (ESI) calculated for $C_{16}H_{15}N_{4+}$ ($[M+H]_+$): 263.12912, found 263.12935.

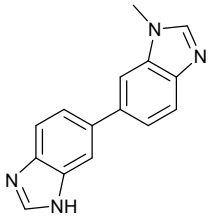

3-methyl-3*H*,3'*H*-5,5'-bibenzo[*d*]imidazole

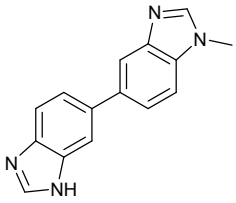

1-methyl-1*H*,3'*H*-5,5'-bibenzo[*d*]imidazole

Light yellow solid (yield: 8%). ^{1}H-NMR (400 MHz, DMSO-d6): δ 8.26 (s, Ar-H), δ 8.21, 8.20 (d, Ar-H), δ 7.88, 7.85 (d Ar-H), δ 7.70-7.53 (m, Ar-H), δ 3.90, 3.87 (d, CH_3) ppm. ^{13}C NMR (101 MHz, DMSO-d6) δ 145.61, 145.45, 144.50, 143.11, 143.00, 142.95, 136.39, 135.95, 135.77, 135.75, 135.73, 134.28, 122.53, 122.14, 122.10, 121.64, 119.88, 117.88, 116.18, 113.75, 110.86, 108.97, 31.18, 31.15 ppm. HMRS (ESI) calculated for $C_{15}H_{13}N_{4+}$ ($[M+H]_+$): 249.11347, found 263.11373.

^{1}H and ^{13}C NMR Spectra of the Products

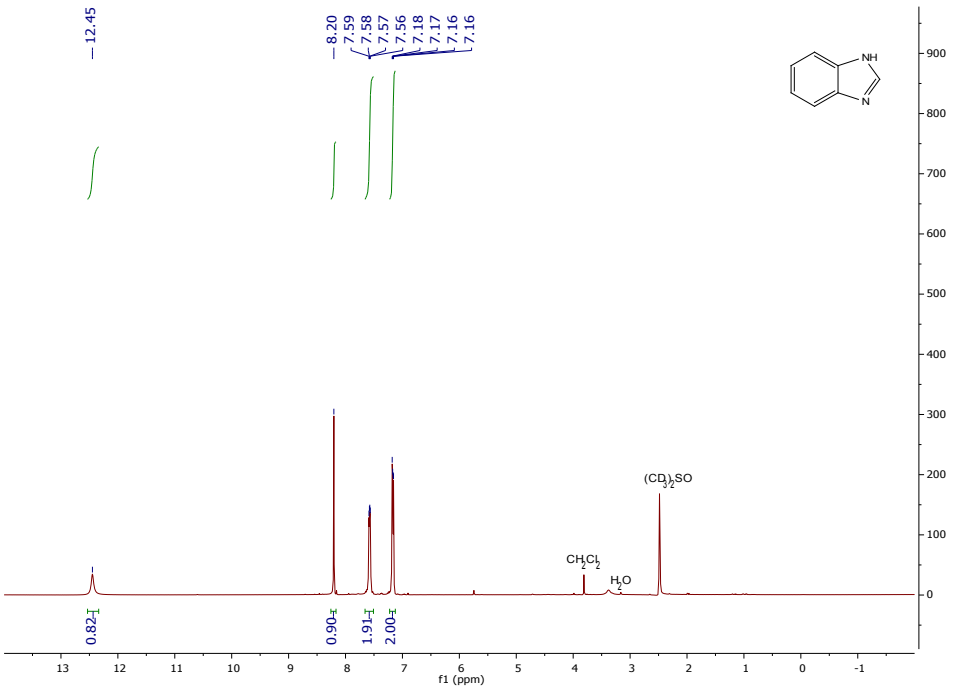

Figure S4. ^{1}H NMR (400 MHz, DMSO-d6) of compound 1a.

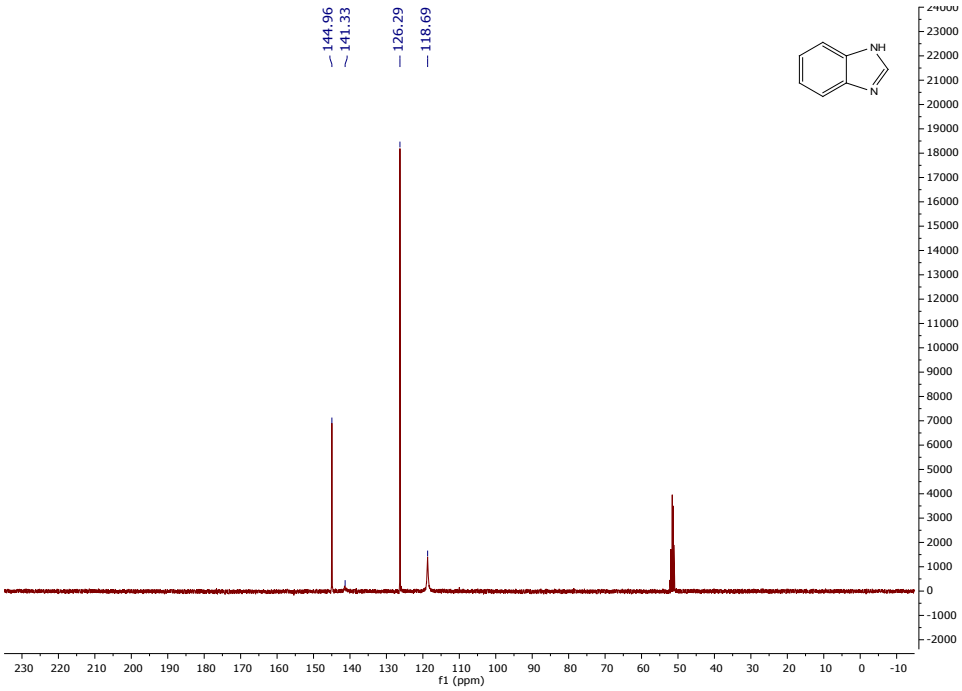

Figure S5. ^{13}C NMR (101 MHz, CD_3OD) of compound 1a.

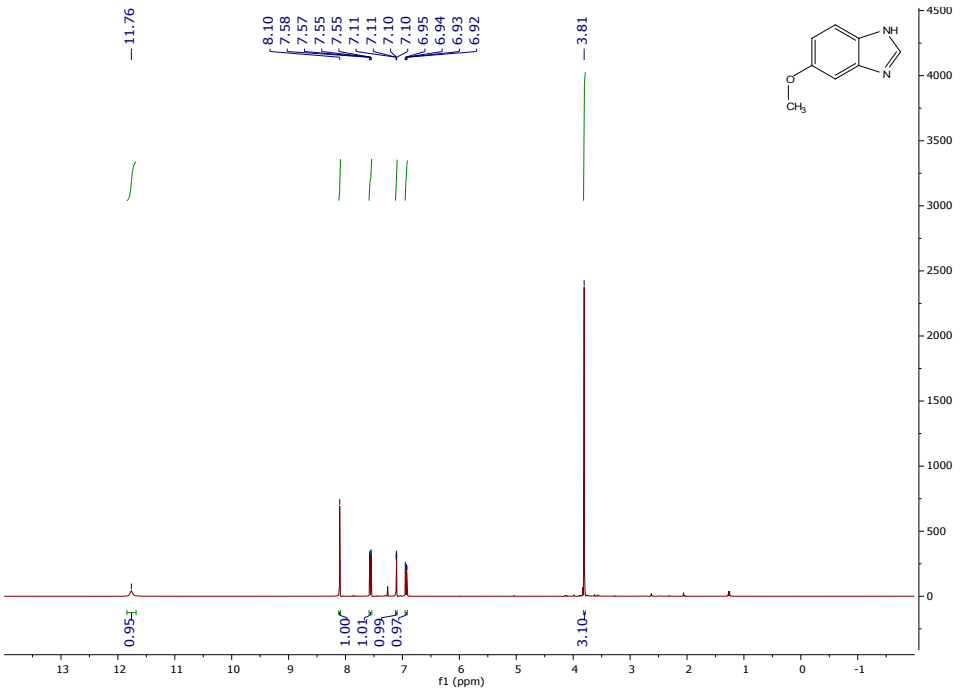

Figure S6. ^{1}H NMR (400 MHz, $CDCl_3$) of compound 2a.

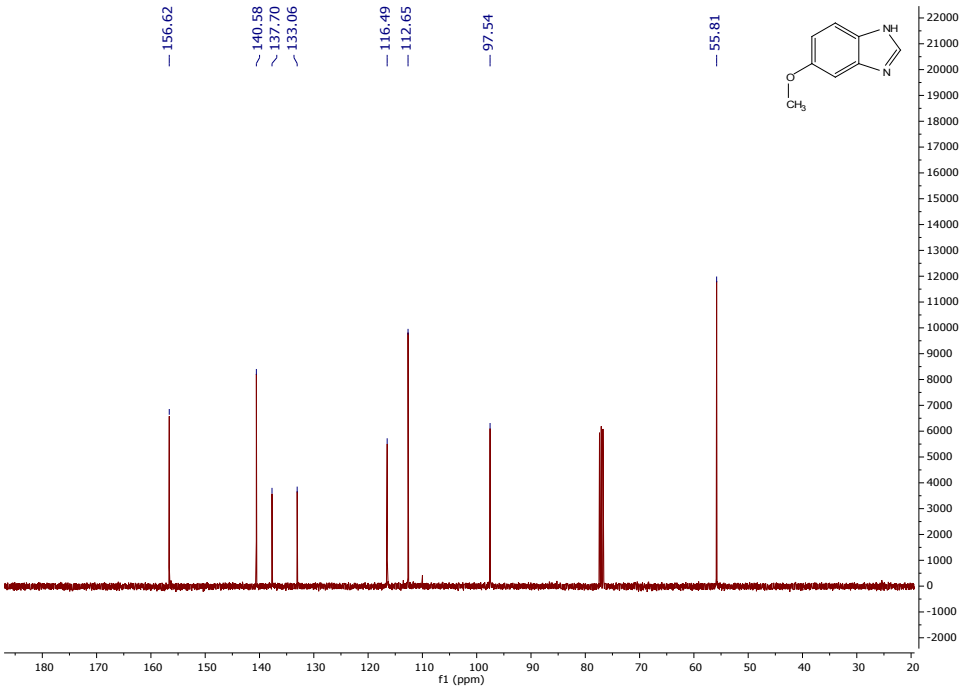

Figure S7. ^{13}C NMR (101MHz, $CDCl_3$) of compound 2a.

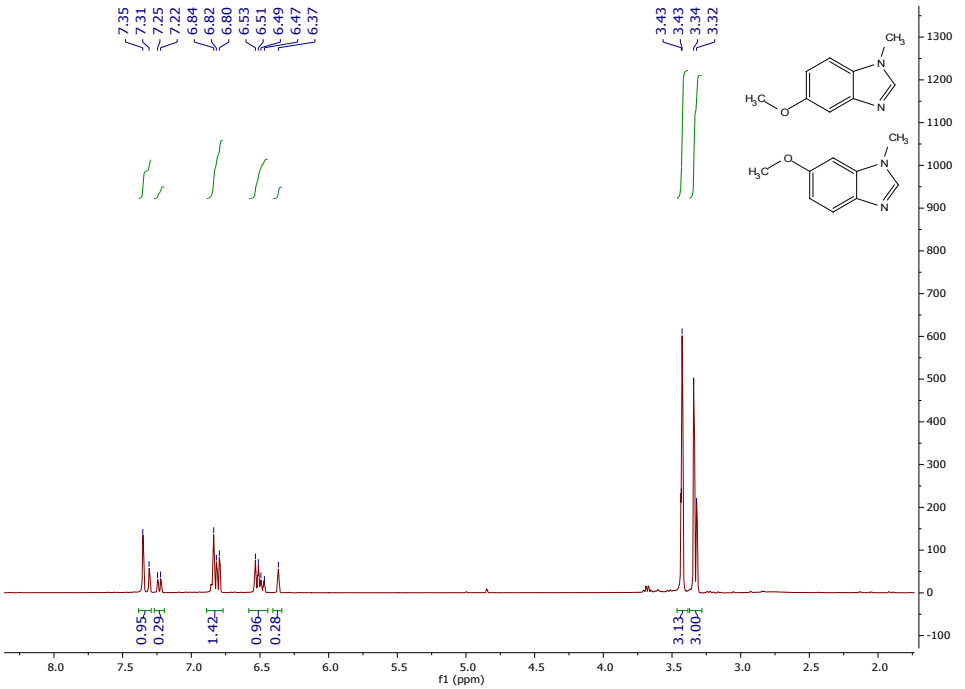

Figure S8. ^{1}H NMR (400 MHz, $CDCl_3$) of compound 2b (isomer ratio of 2.4:1)

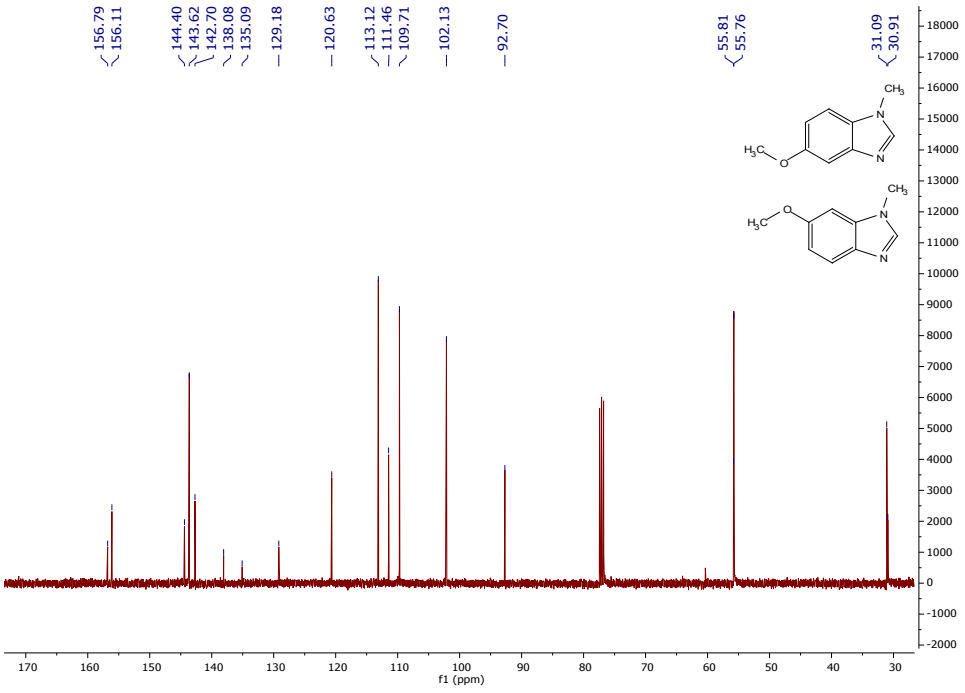

Figure S9. ^{13}C NMR (101MHz, $CDCl_3$) of compound 2b (isomer ratio of 2.4:1).

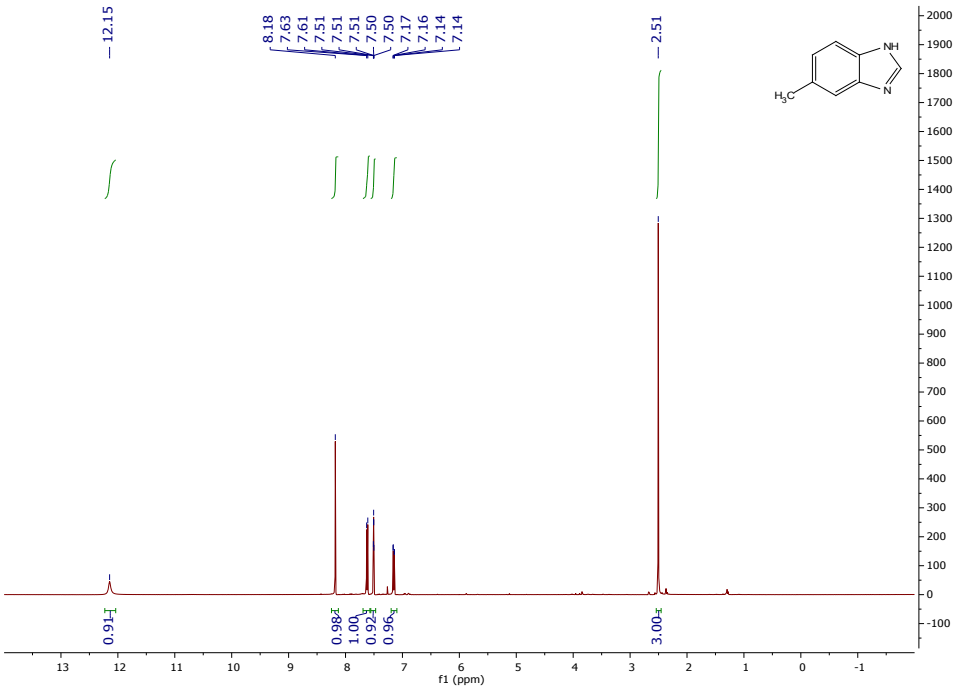

Figure S10. ^{1}H NMR (400 MHz, $CDCl_3$) of compound 3a.

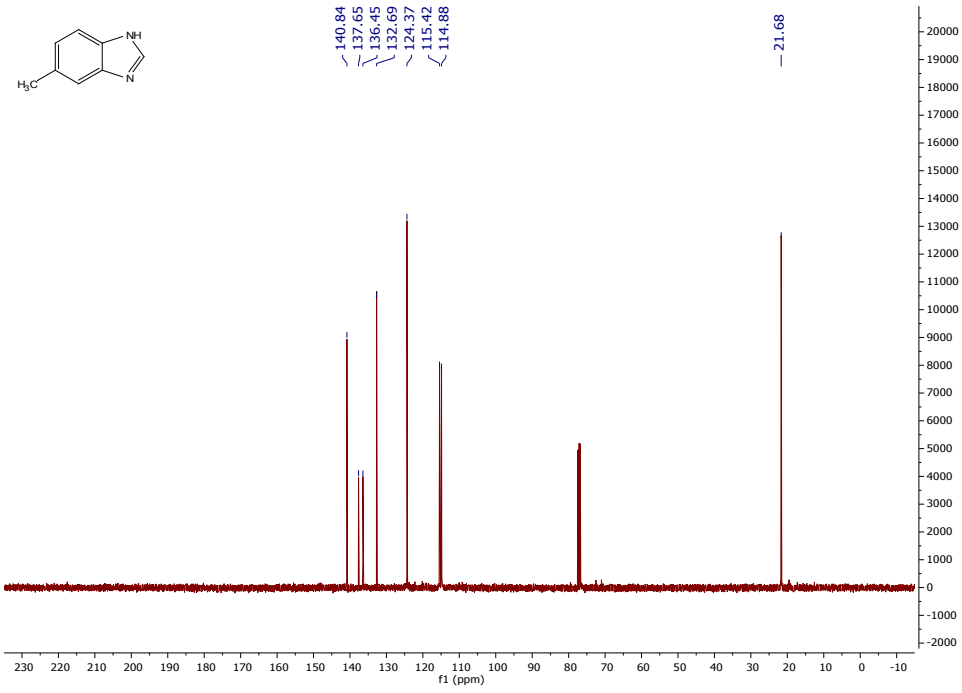

Figure S11. ^{13}C NMR (101 MHz, $CDCl_3$) of compound 3a.

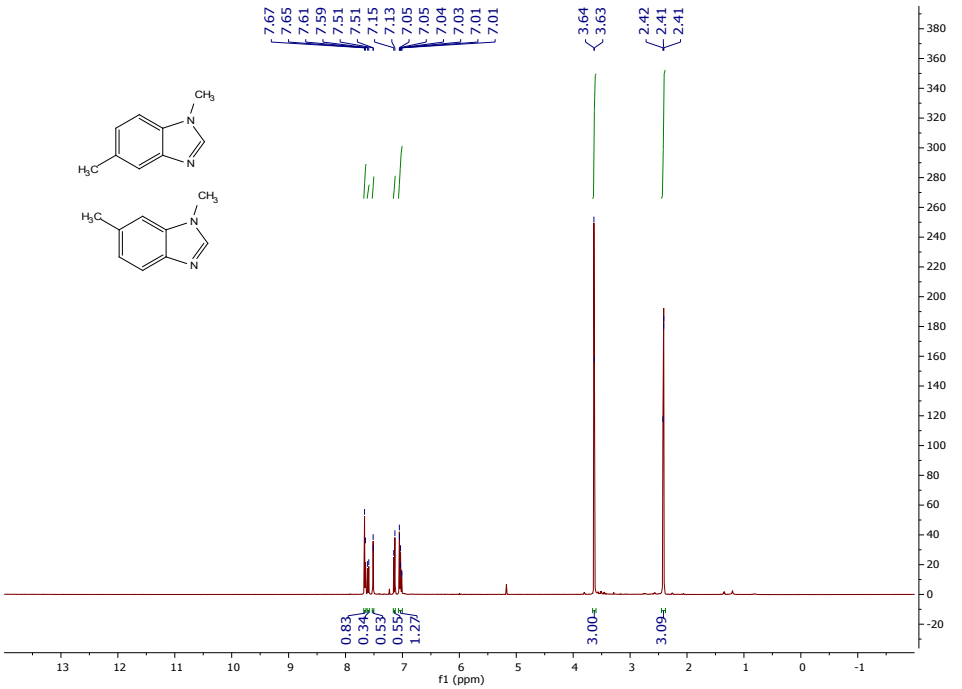

Figure S12. ^{1}H NMR (400 MHz, $CDCl_3$) of compound 3b (isomer ratio of 1.6:1).

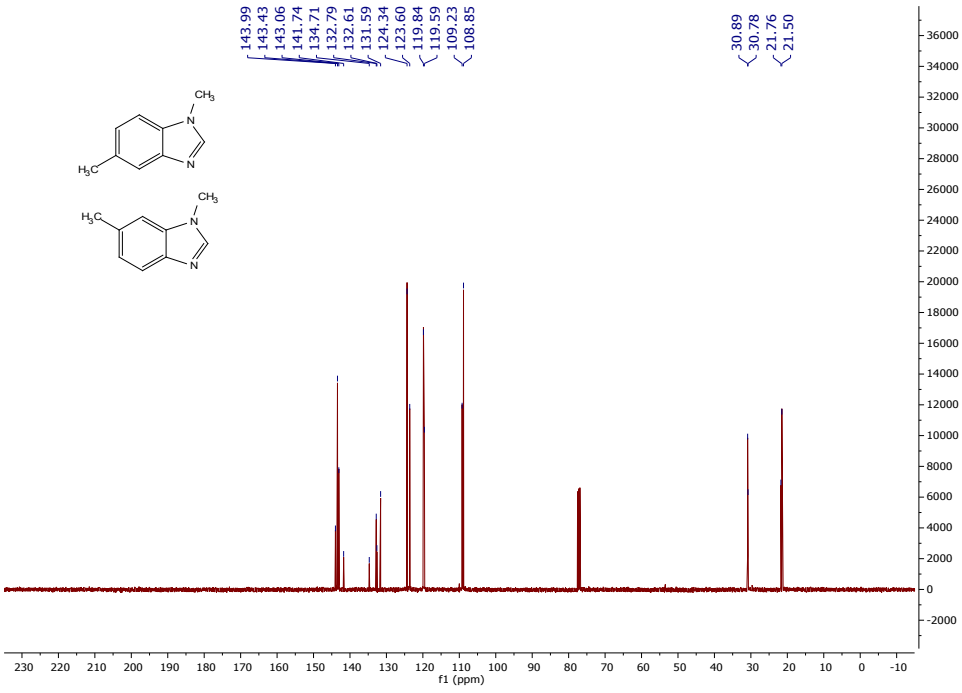

Figure S13. ^{13}C NMR (101 MHz, $CDCl_3$) of compound 3b (isomer ratio of 1.6:1).

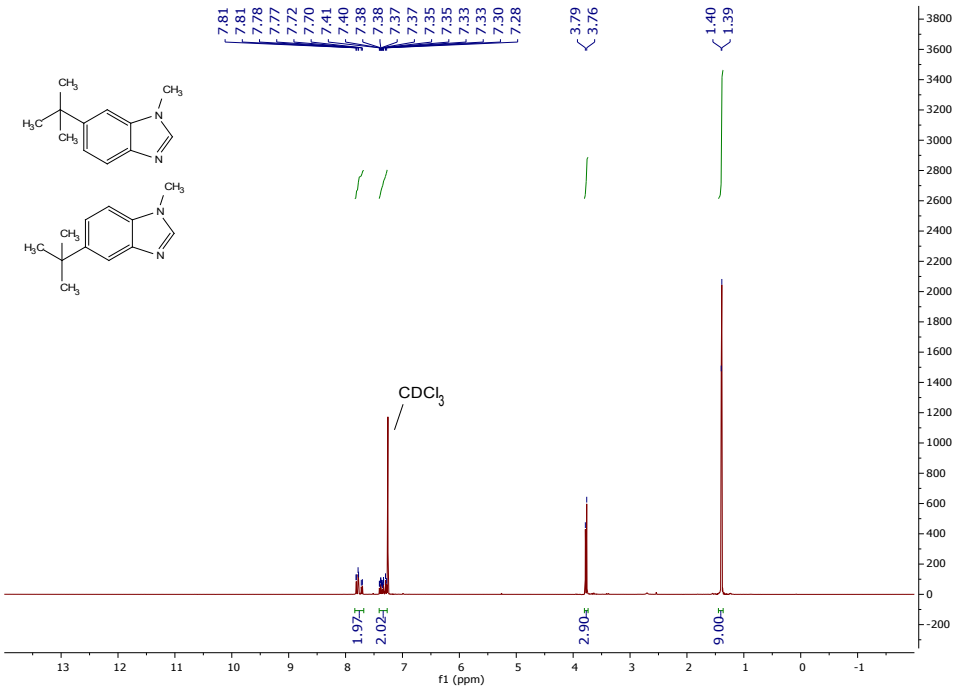

Figure S14. ^{1}H NMR (400 MHz, $CDCl_3$) of compound 4b (isomer ratio of 1.4:1).

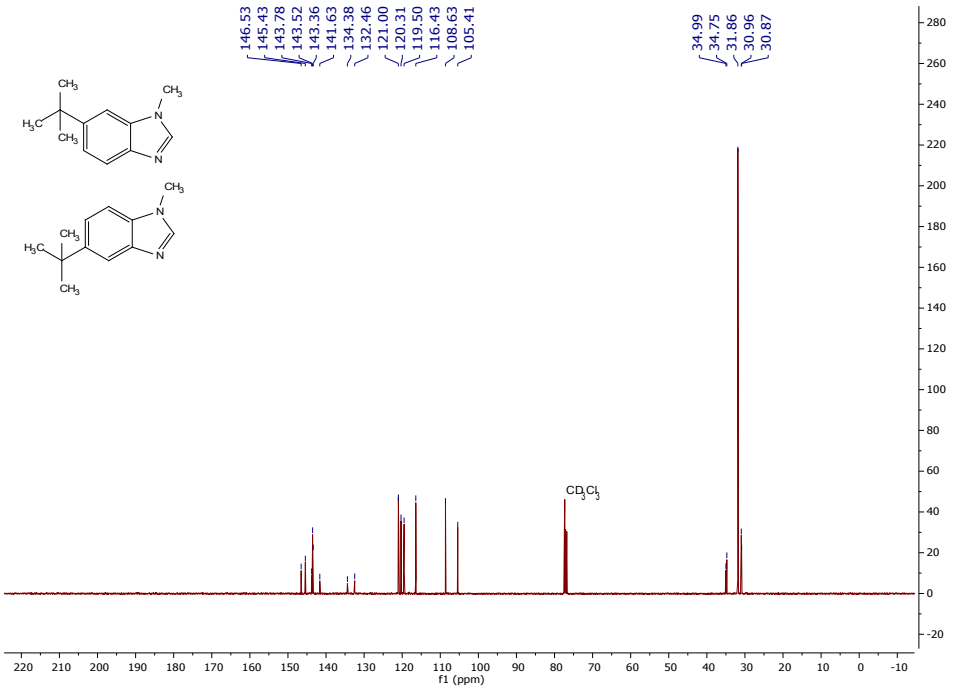

Figure S15. ^{13}C NMR (101 MHz, $CDCl_3$) of compound 4b (isomer ratio of 1.4:1).

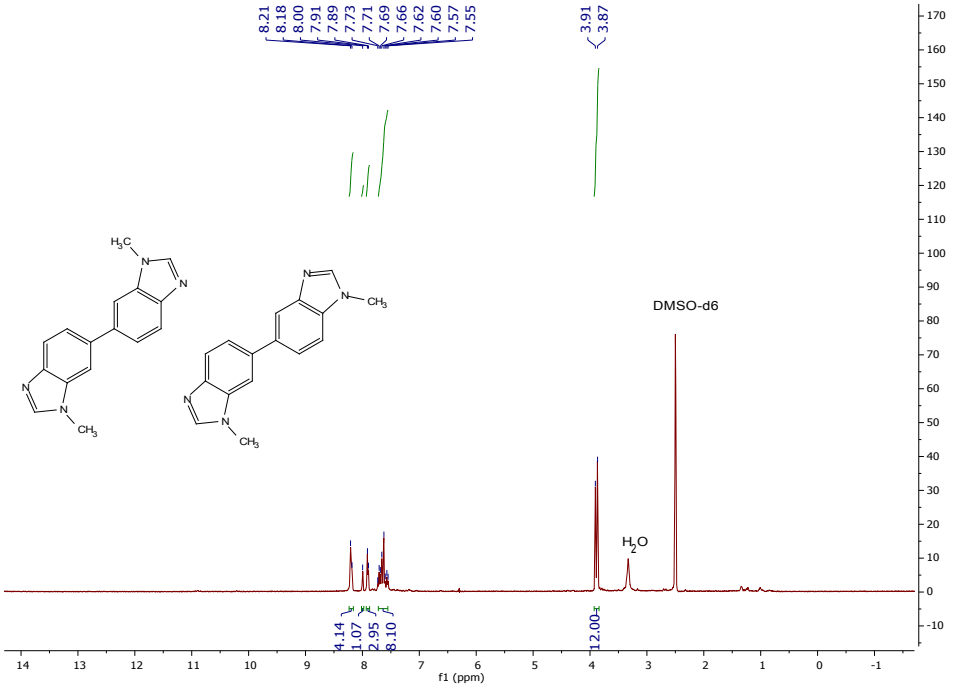

Figure S16. ^{1}H NMR (400 MHz, DMSO-d6) of compound 5a (isomer ratio of 1.3:1).

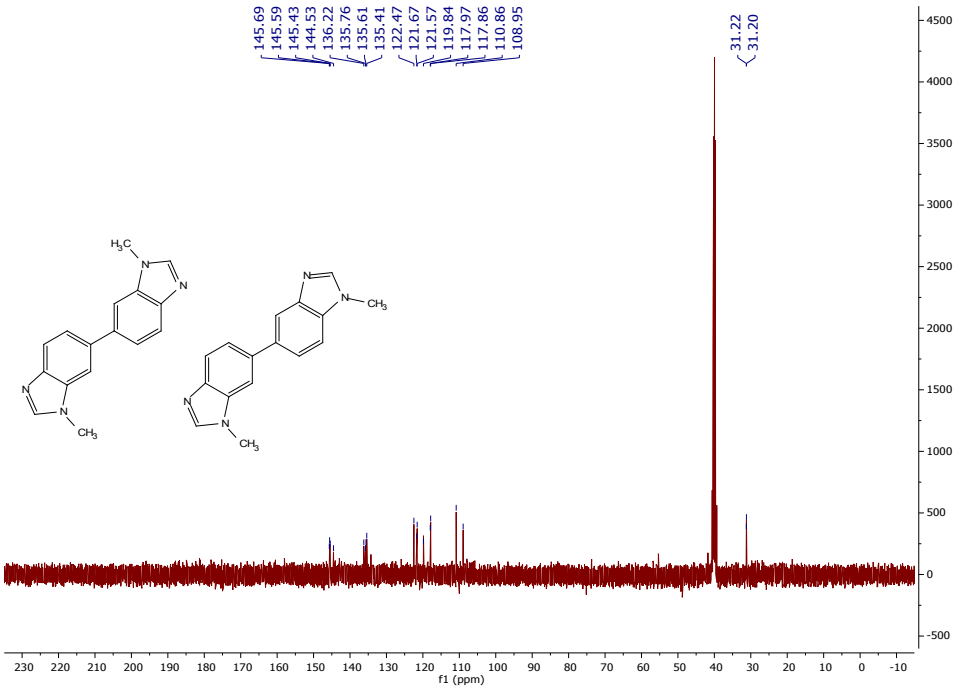

Figure S17. ^{13}C NMR (101 MHz, DMSO-d6) of compound 5a (isomer ratio of 1.3:1).

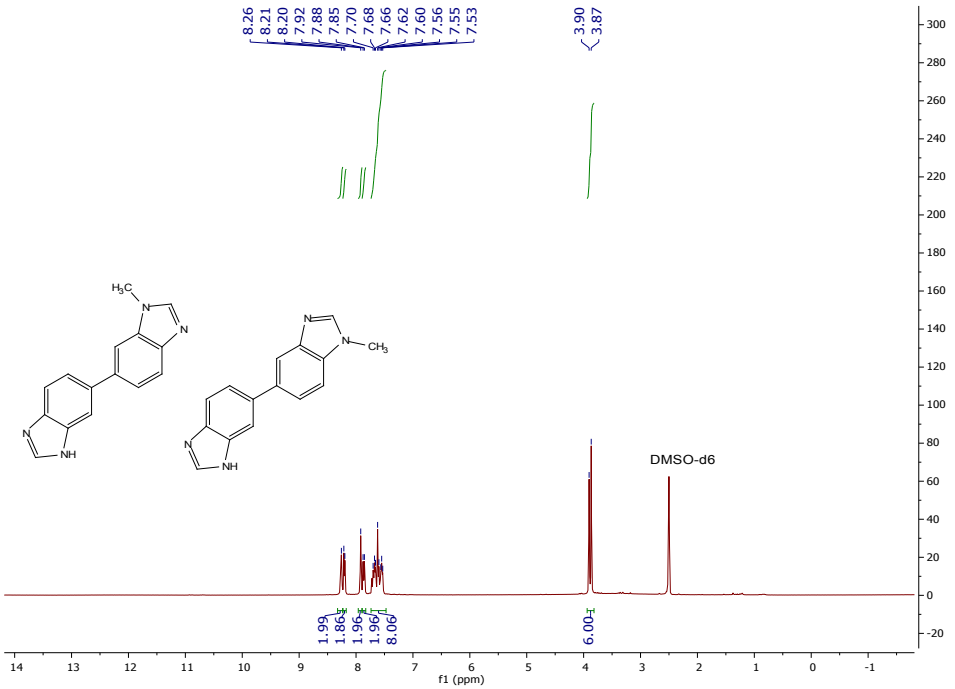

Figure S18. ^{1}H NMR (400 MHz, DMSO-d6) of compound 5b (isomer ratio of 1.2:1).

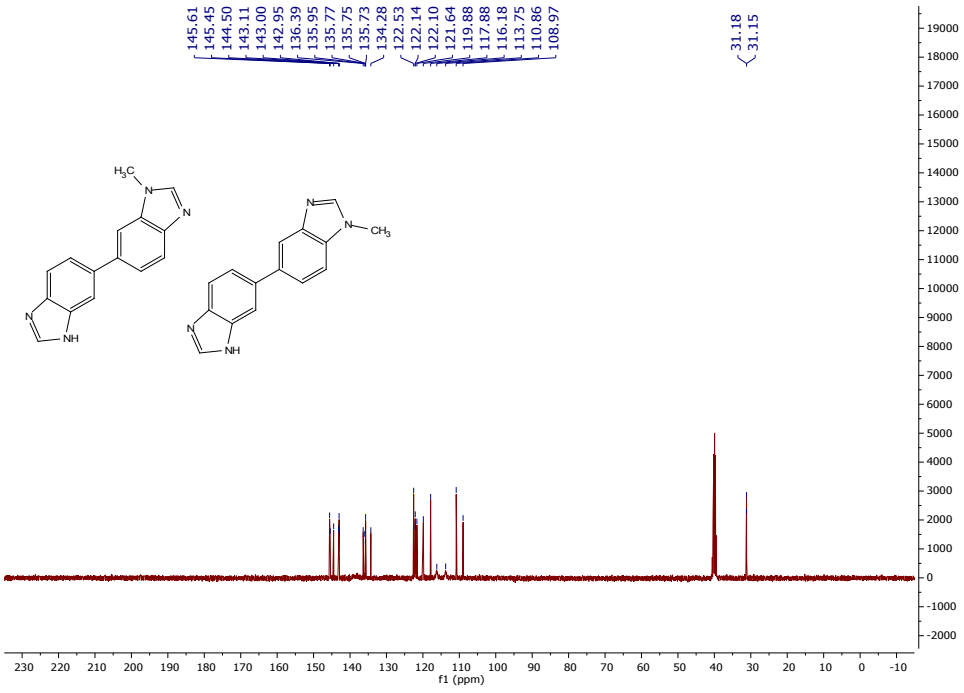

Figure S19. ^{13}C NMR (101 MHz, DMSO-d6) of compound 5b (isomer ratio of 1.2:1).

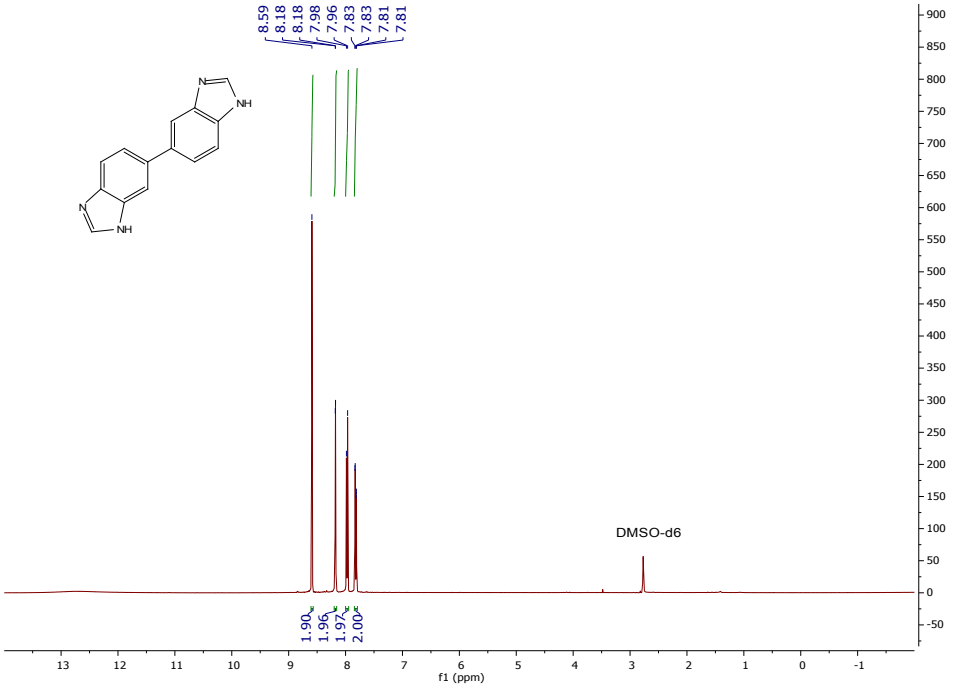

Figure S20. ^{1}H NMR (400 MHz, DMSO-d6) of compound 5c.

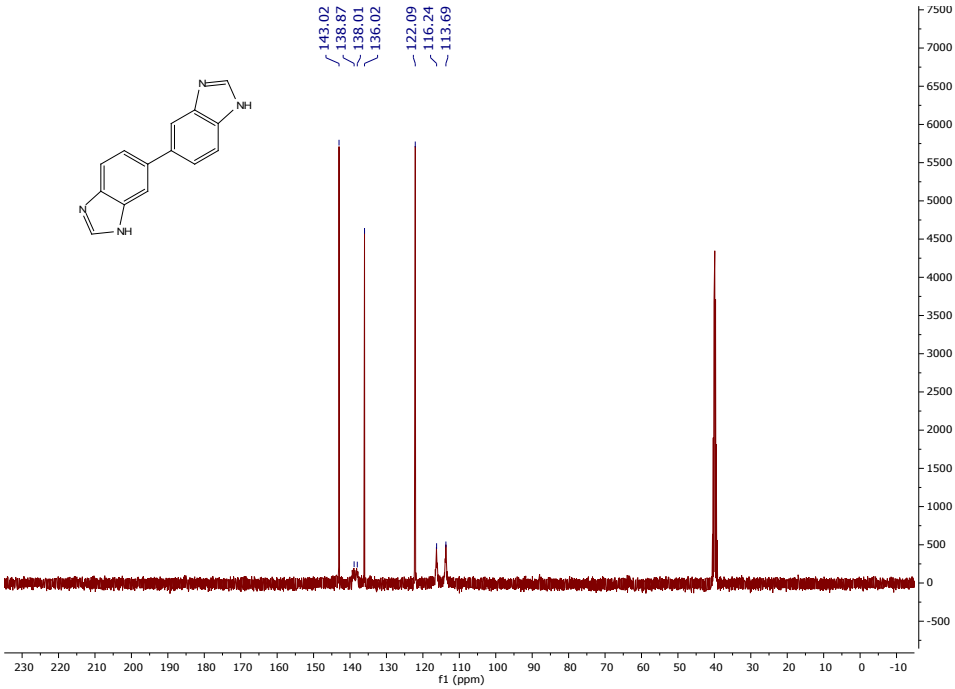

Figure S21. ^{13}C NMR (101 MHz, DMSO-d6) of compound 5c.

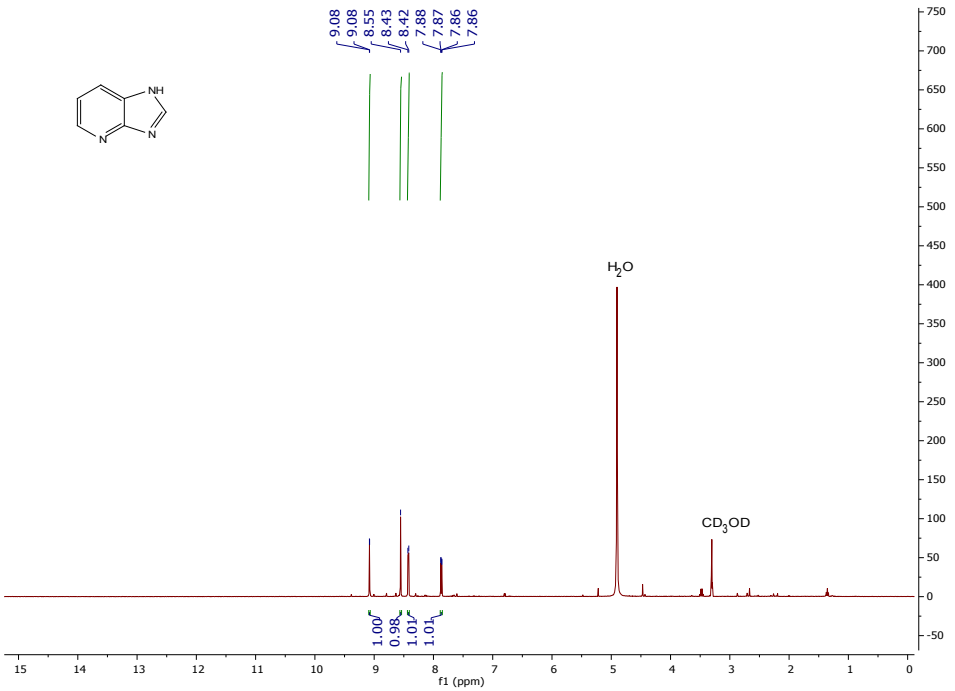

Figure S22. ^{1}H NMR (400 MHz, CD_3OD) of compound 6a.

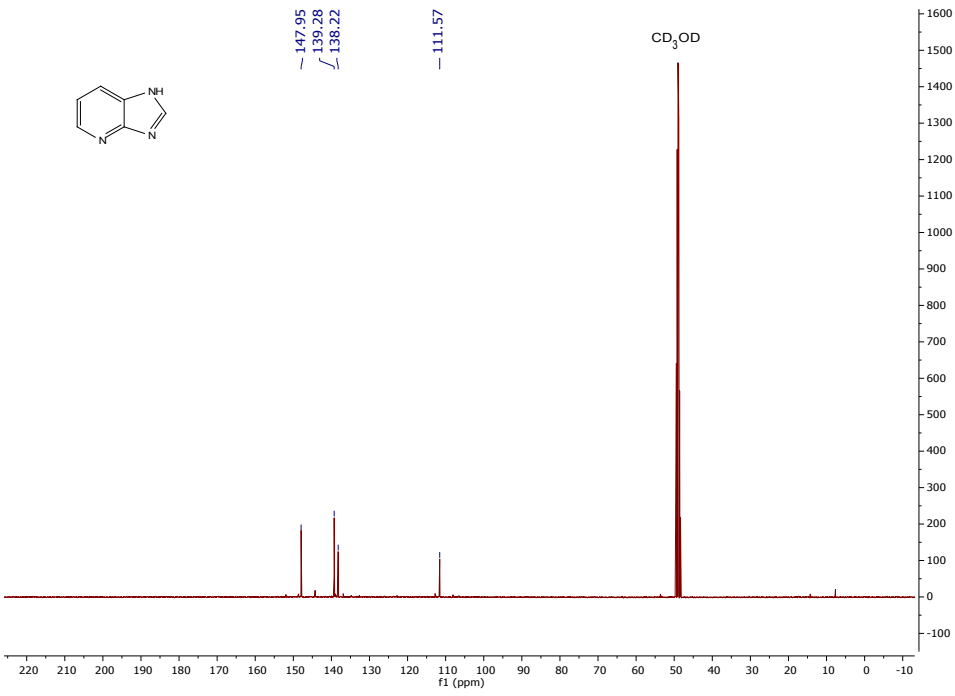

Figure S23. ^{12}C NMR (101 MHz, CD_3OD) of compound 6a.

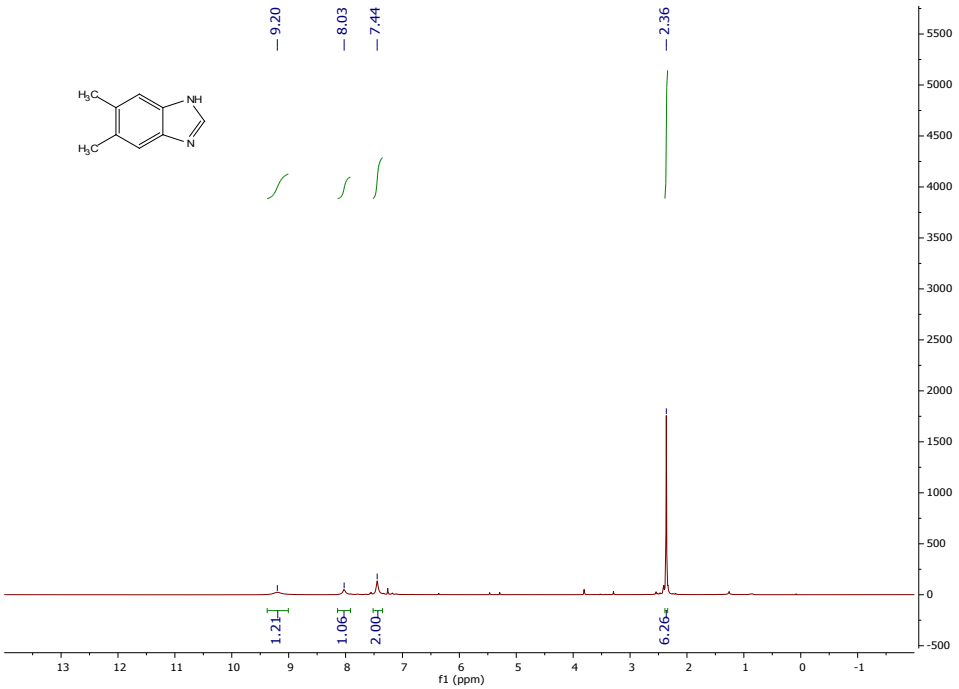

Figure S24. ^{1}H NMR (400 MHz, $CDCl_3$) of compound 10a.

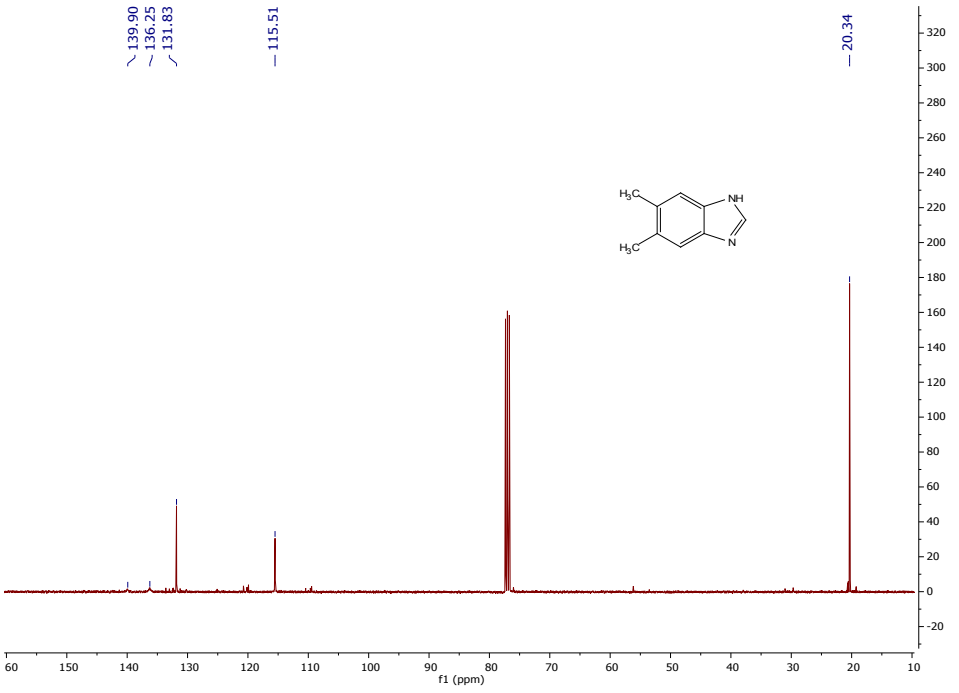

Figure S25. ^{13}C NMR (101 MHz, $CDCl_3$) of compound 10a.

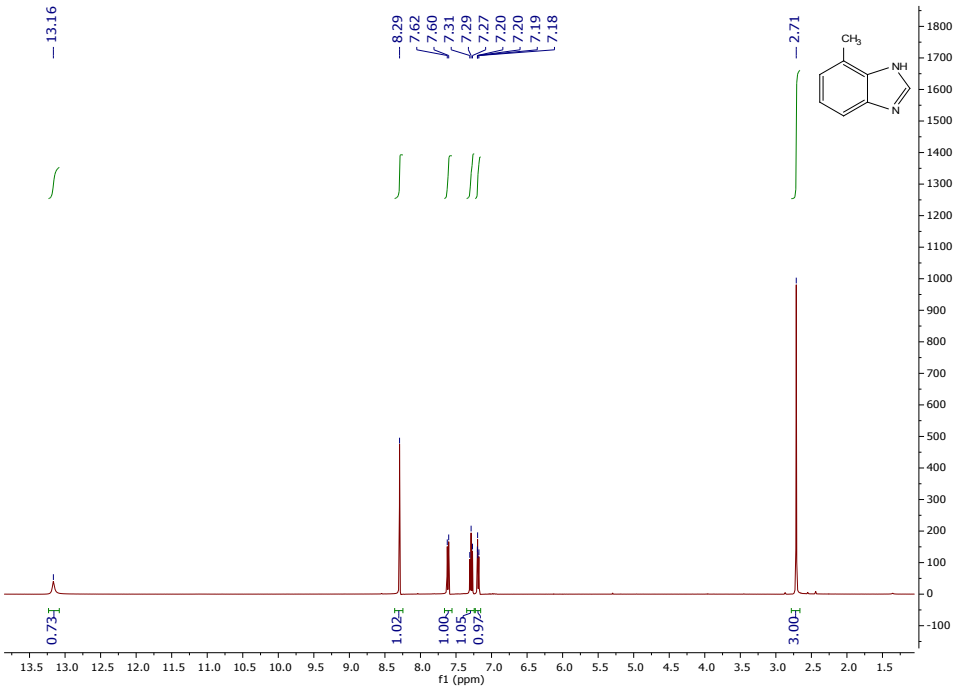

Figure S26. ^{1}H NMR (400 MHz, $CDCl_3$) of compound 12a.

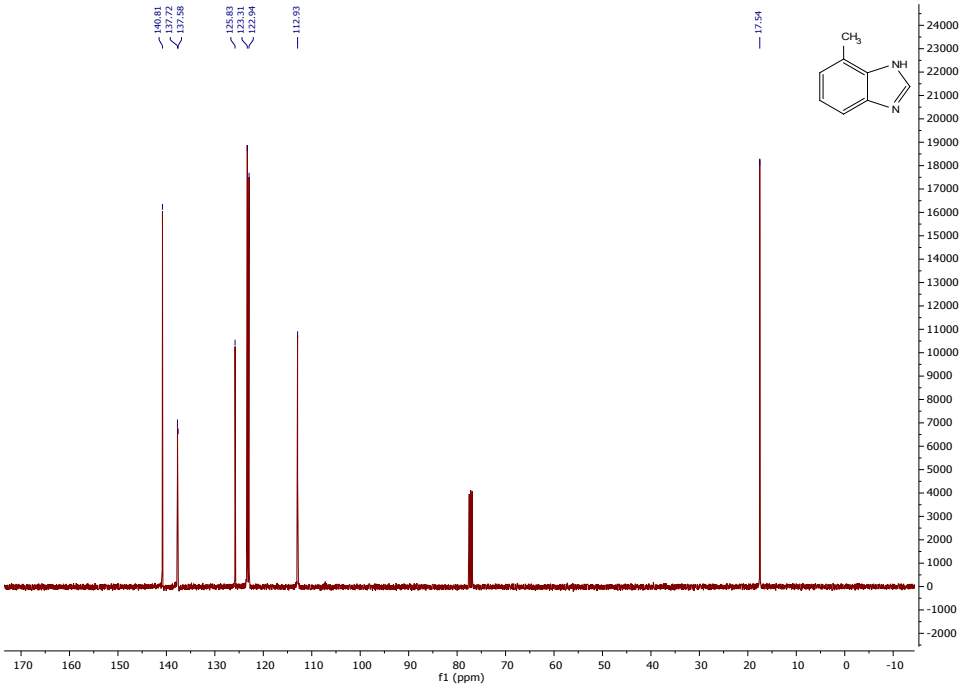

Figure S27. ^{13}C NMR (101 MHz, $CDCl_3$) of compound 12a.

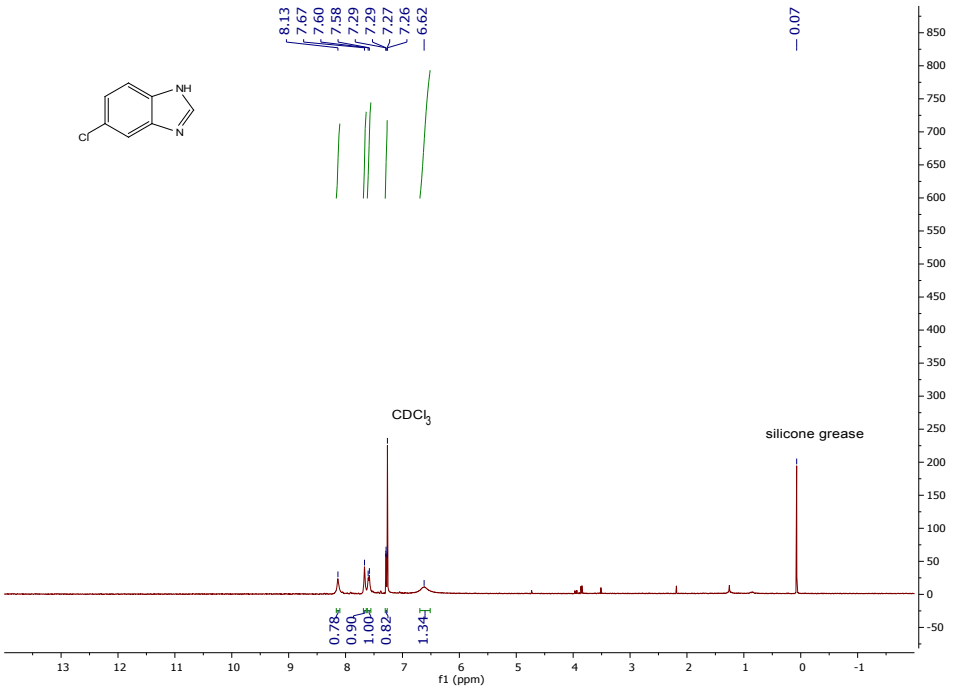

Figure S28. ^{1}H NMR (400 MHz, $CDCl_3$) of compound 13a.

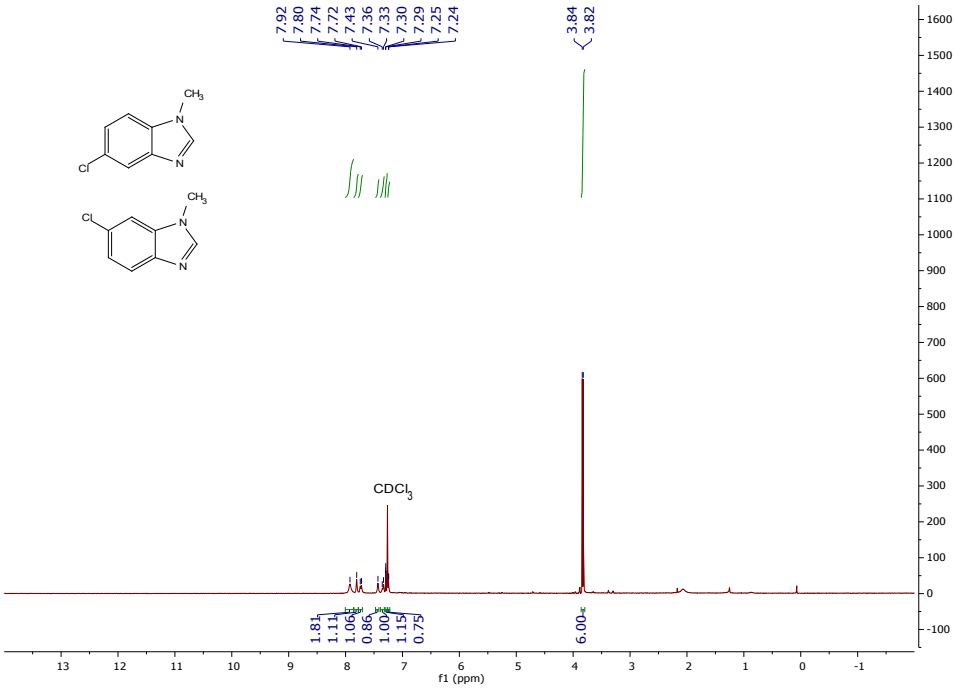

Figure S29. ^{1}H NMR (400 MHz, $CDCl_3$) of compound 13b (isomer ratio of 1:1).

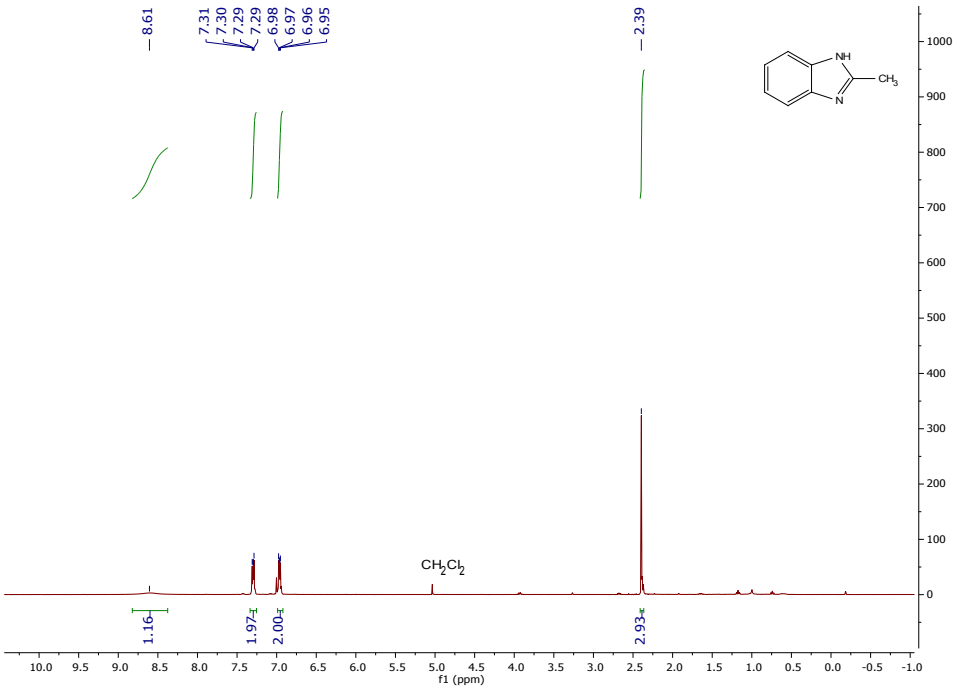

Figure S30. ^{1}H NMR (400 MHz, $CDCl_3$) of compound 14a.

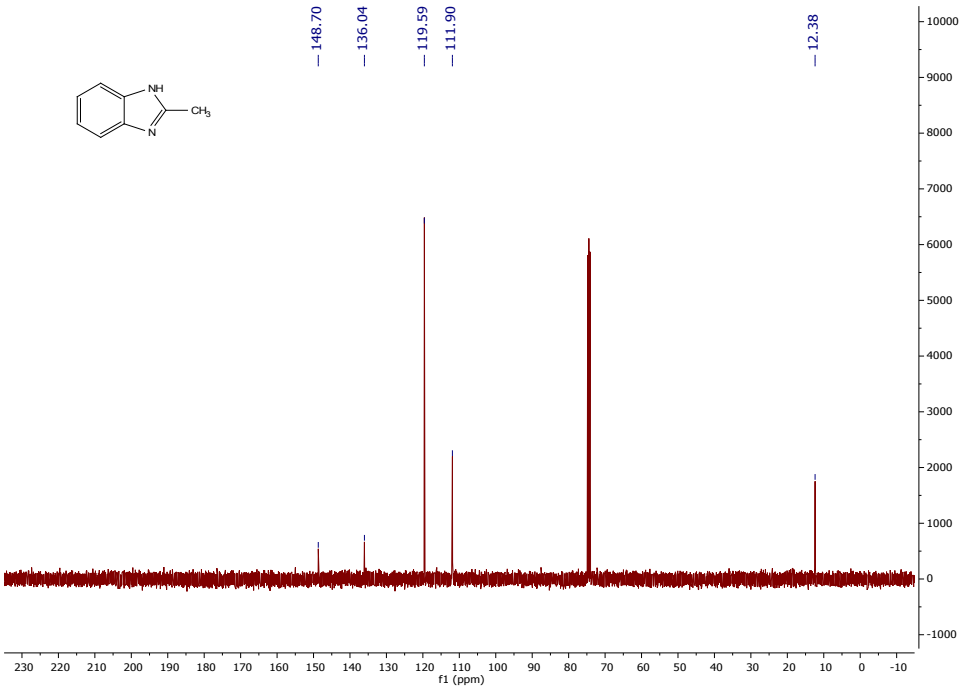

Figure S31. ^{13}C NMR (101 MHz, $CDCl_3$) of compound 14a.

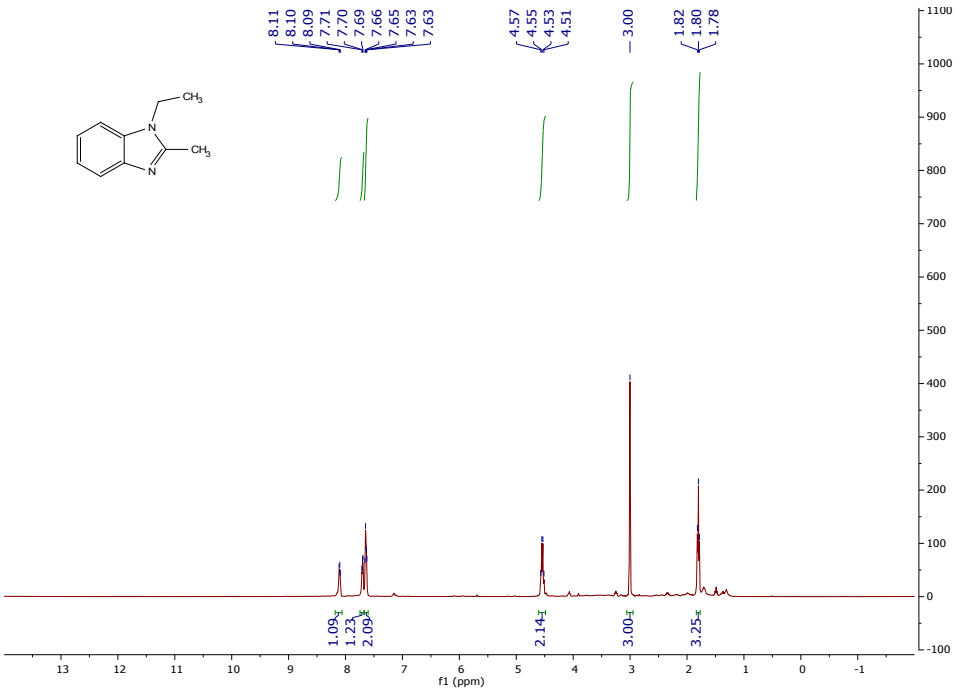

Figure S32. ^{1}H NMR (400 MHz, $CDCl_3$) of compound 14b.

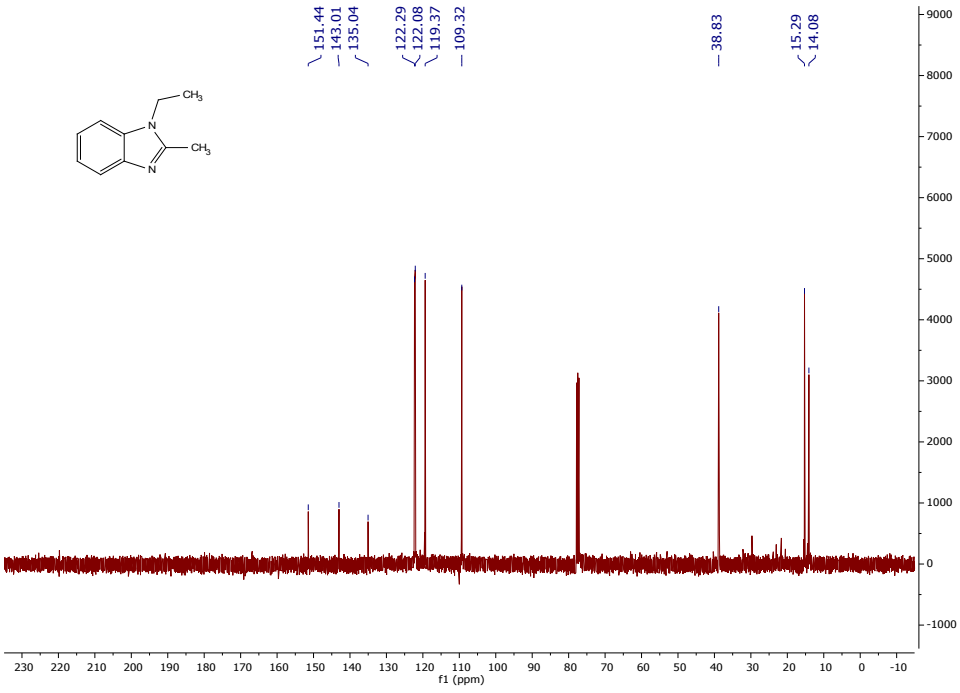

Figure S33. ^{13}C NMR (101 MHz, $CDCl_3$) of compound 14b.

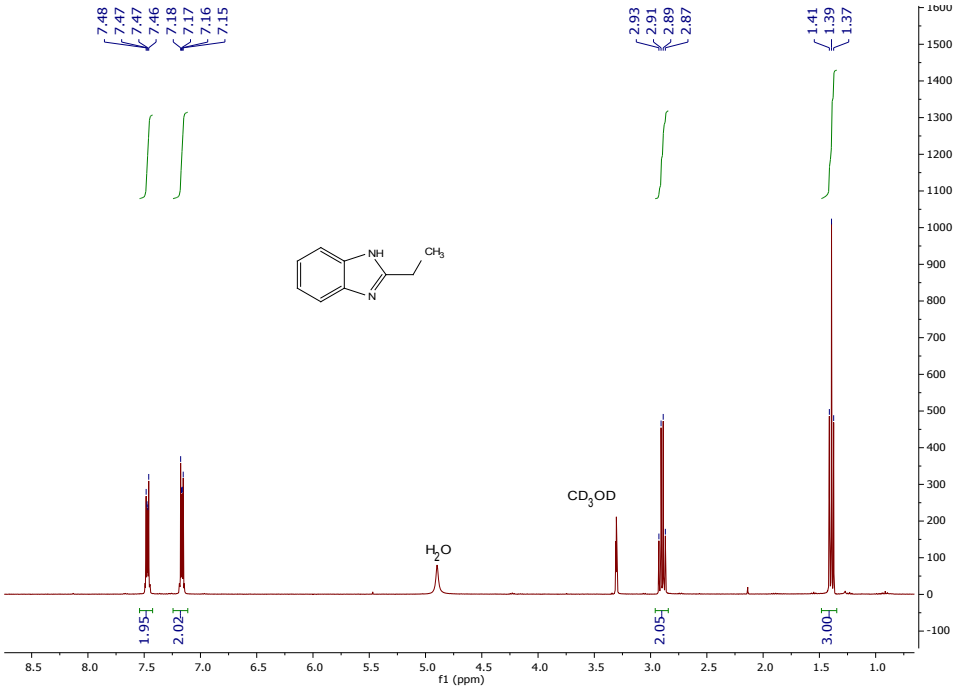

Figure S34. ^{1}H NMR (400 MHz, CD_3OD) of compound 15a.

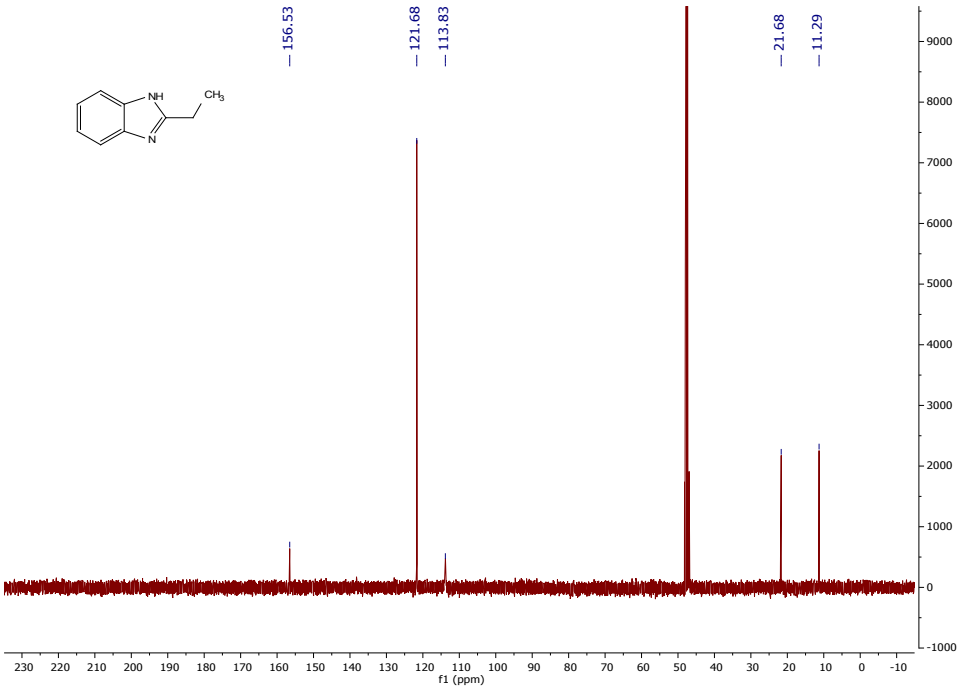

Figure S35. ^{13}C NMR (101 MHz, CD_3OD) of compound 15a.

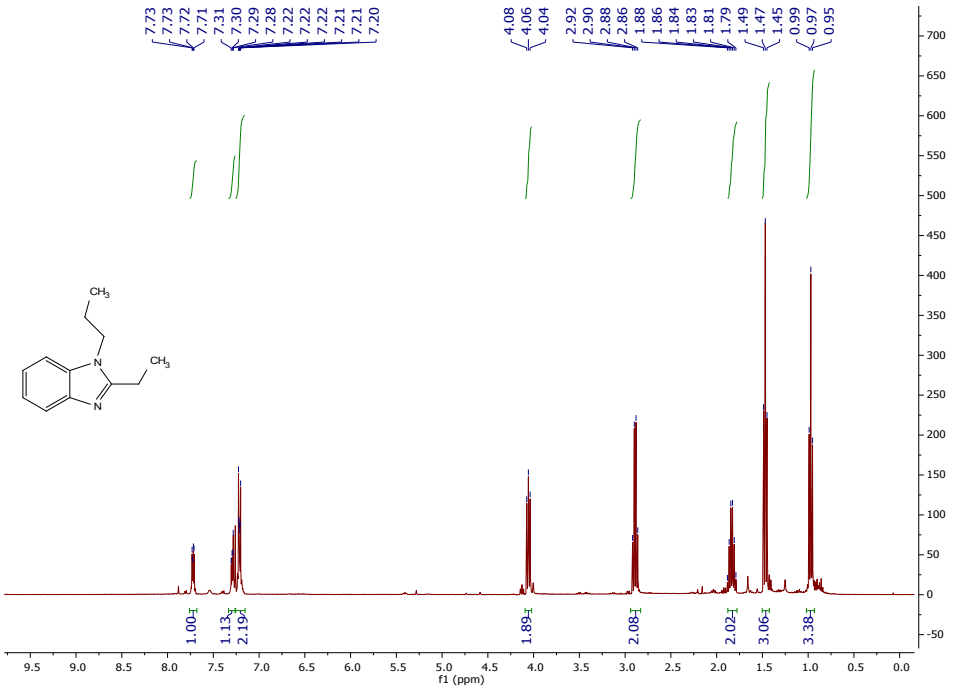

Figure S36. ^{1}H NMR (400 MHz, CD_3OD) of compound 15b.

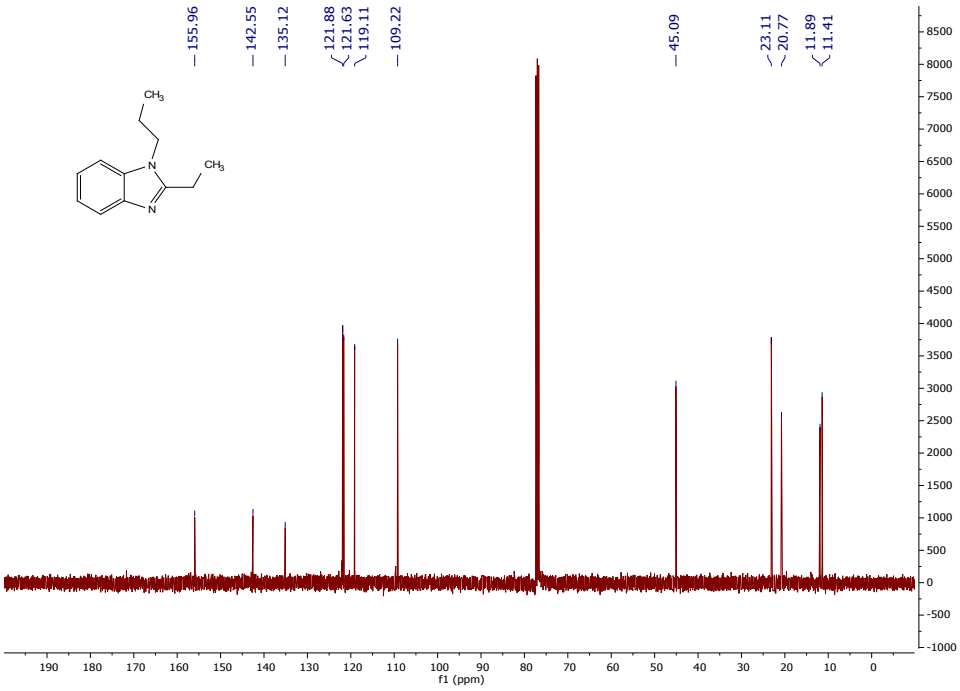

Figure S37. ^{13}C NMR (101 MHz, CD_3OD) of compound 15b.

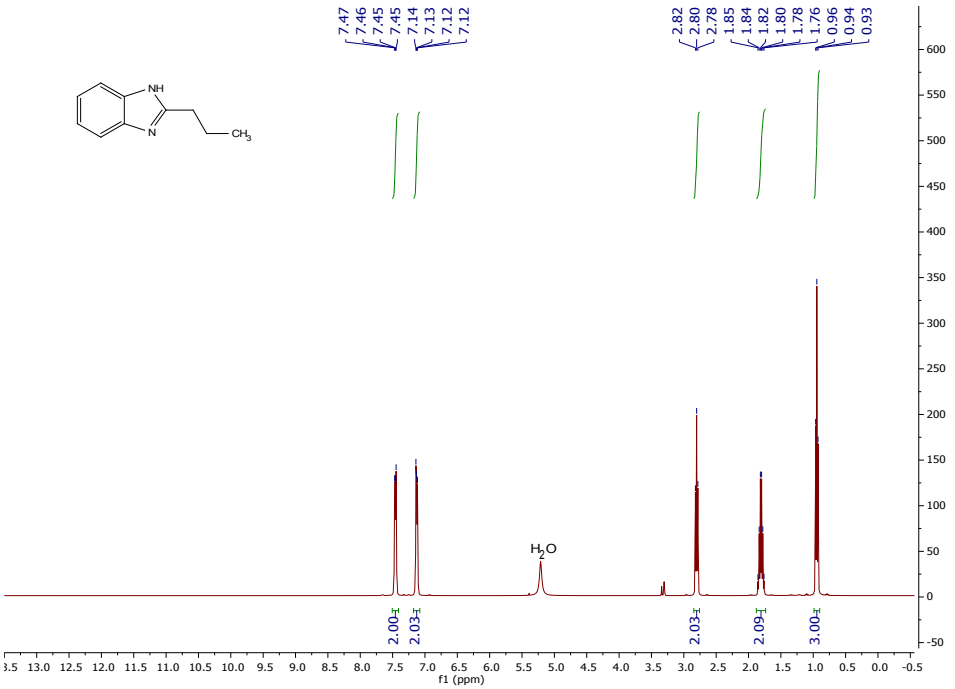

Figure S38. ^{1}H NMR (400 MHz, CD_3OD) of compound 16a.

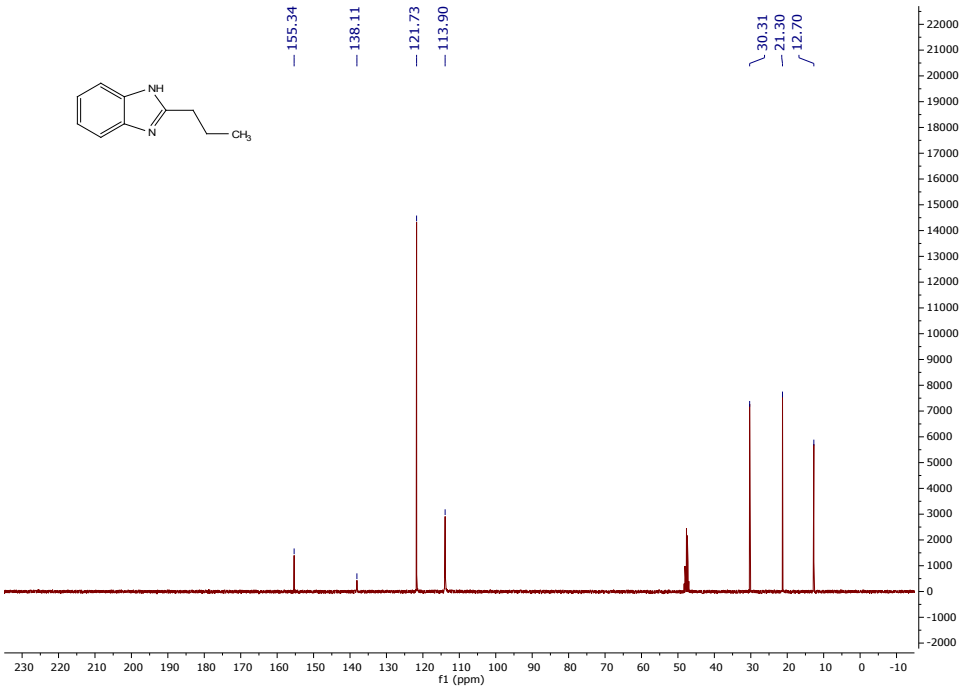

Figure S39. ^{13}C NMR (101 MHz, CD_3OD) of compound 16a.

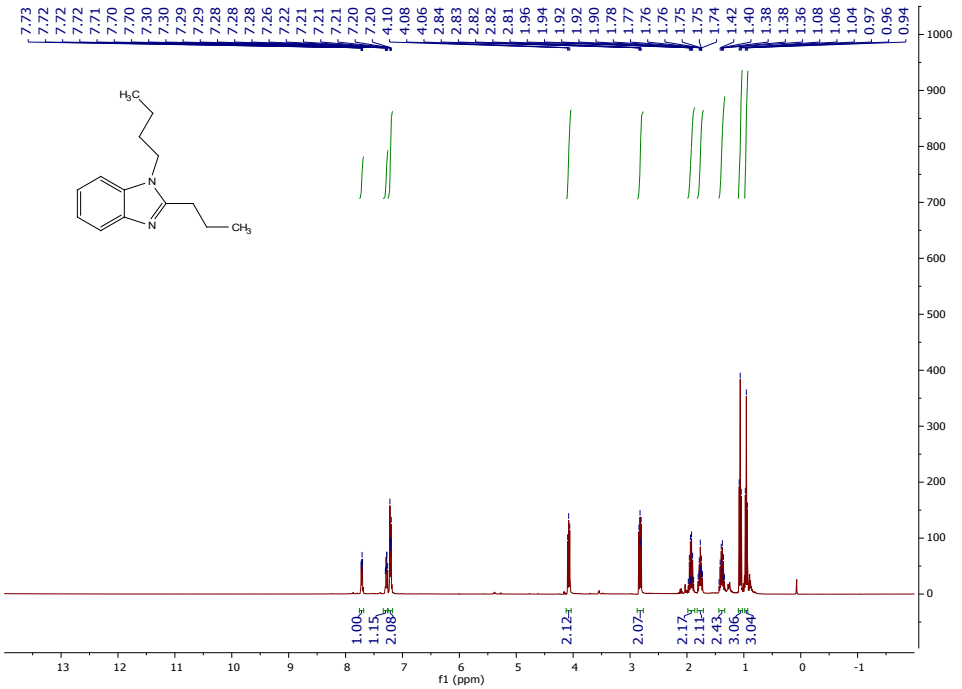

Figure S40. ^{1}H NMR (400 MHz, $CDCl_3$) of compound 16b.

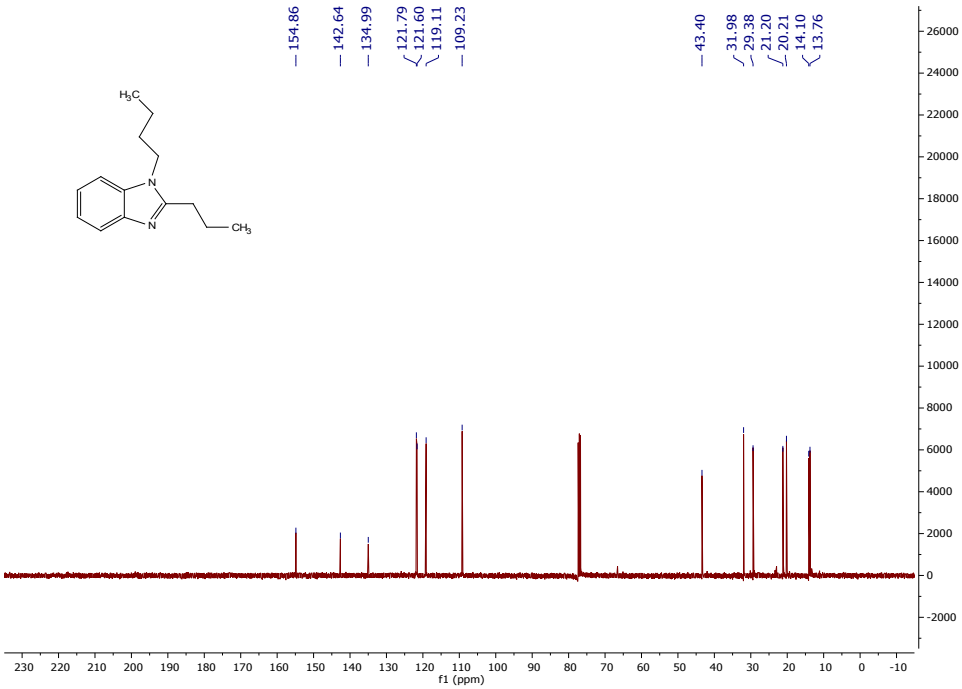

Figure S41. ^{13}C NMR (101 MHz, $CDCl_3$) of compound 16b.

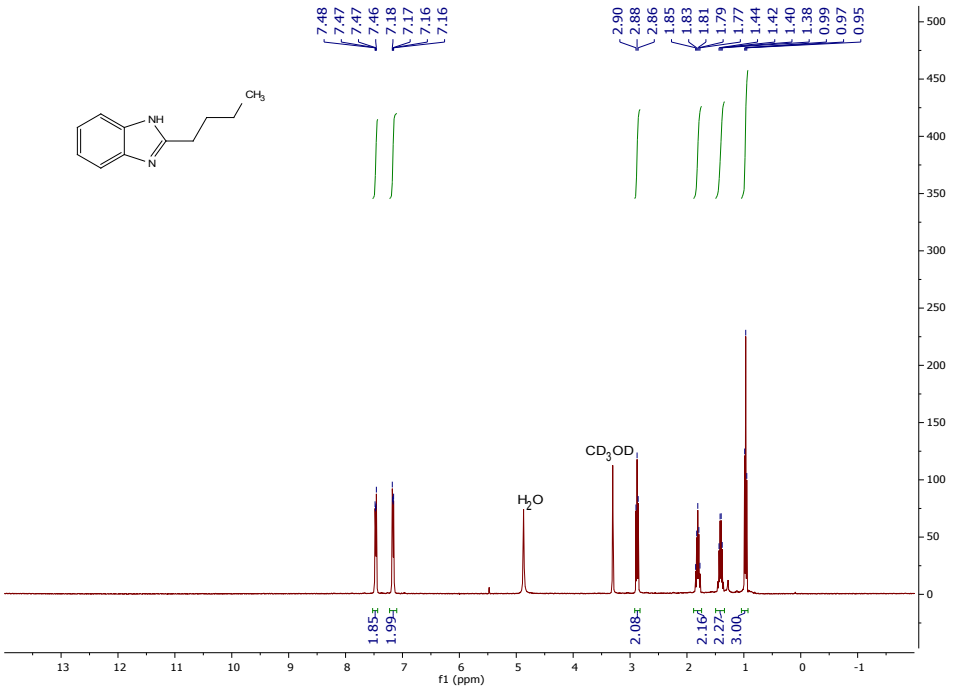

Figure S42. ^{1}H NMR (400 MHz, CD_3OD) of compound 17a.

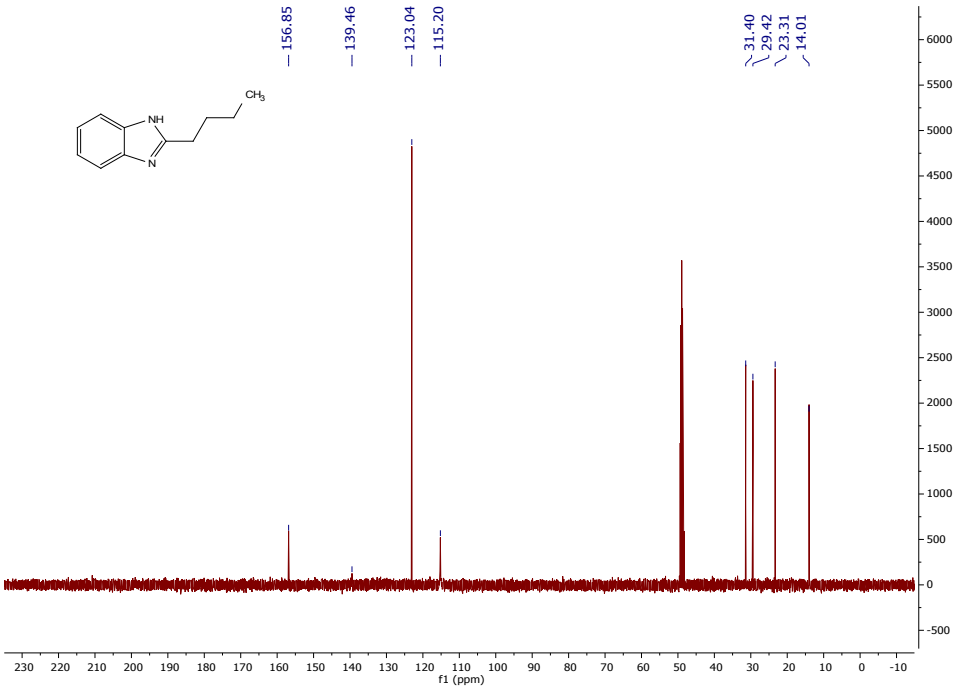

Figure S43. ^{13}C NMR (101 MHz, CD_3OD) of compound 17a.

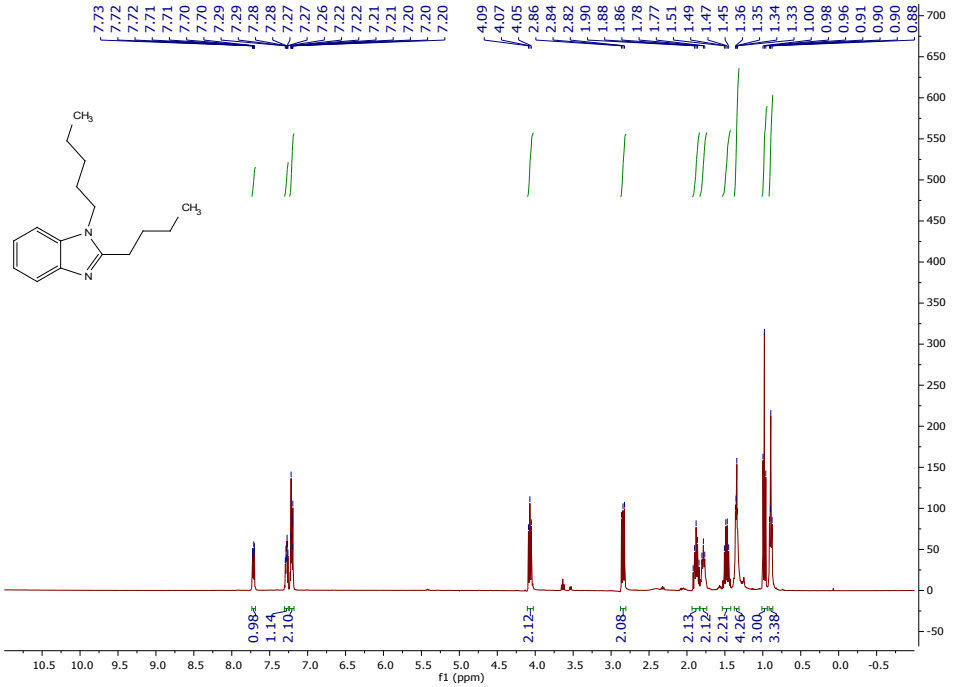

Figure S44. ^{1}H NMR (400 MHz, CD_3OD) of compound 17b.

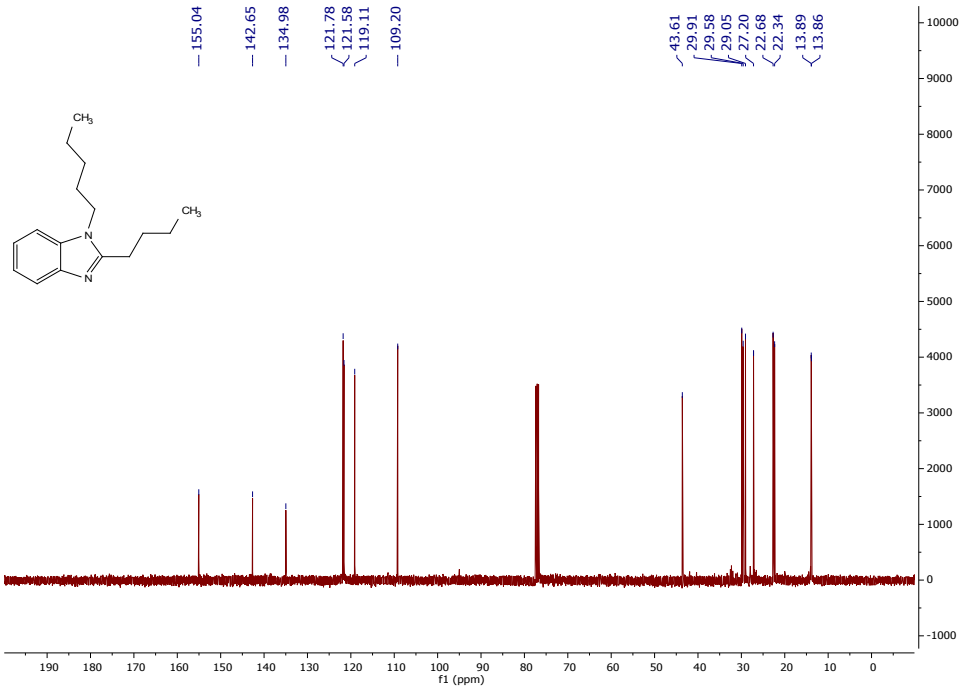

Figure S45. ^{13}C NMR (101 MHz, $CDCl_3$) of compound 17b.

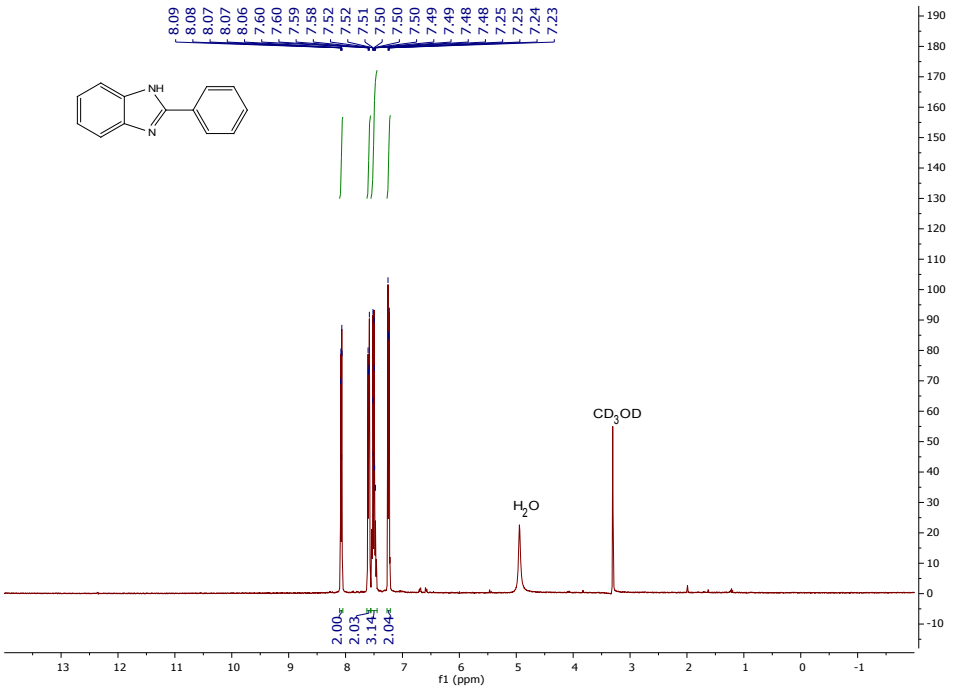

Figure S46. ^{1}H NMR (400 MHz, CD_3OD) of compound 18a.

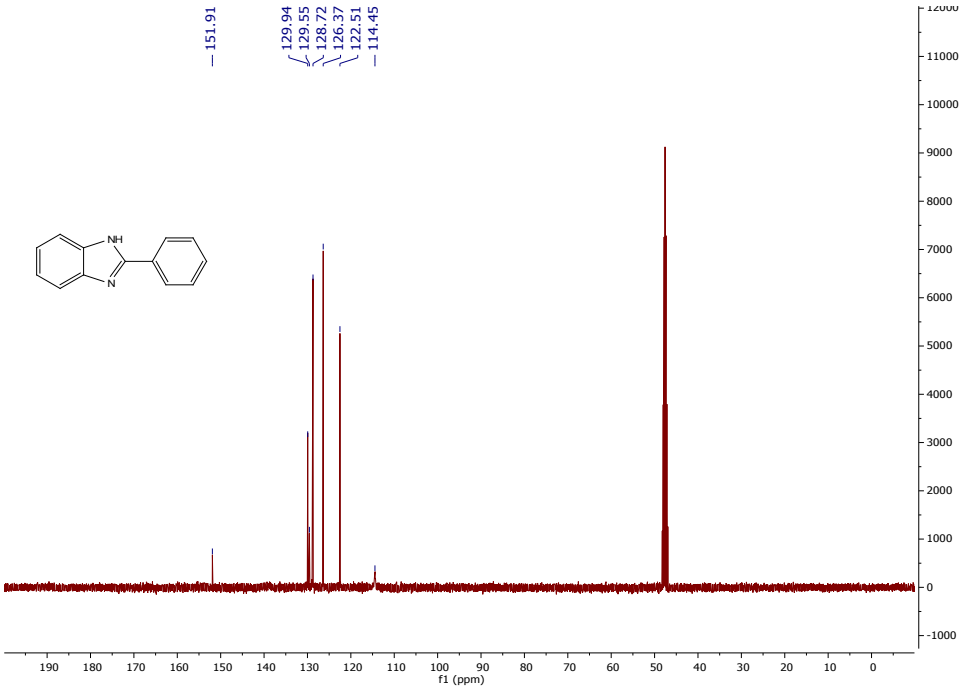

Figure S47. ^{13}C NMR (101 MHz, $CDCl_3$) of compound 18a.

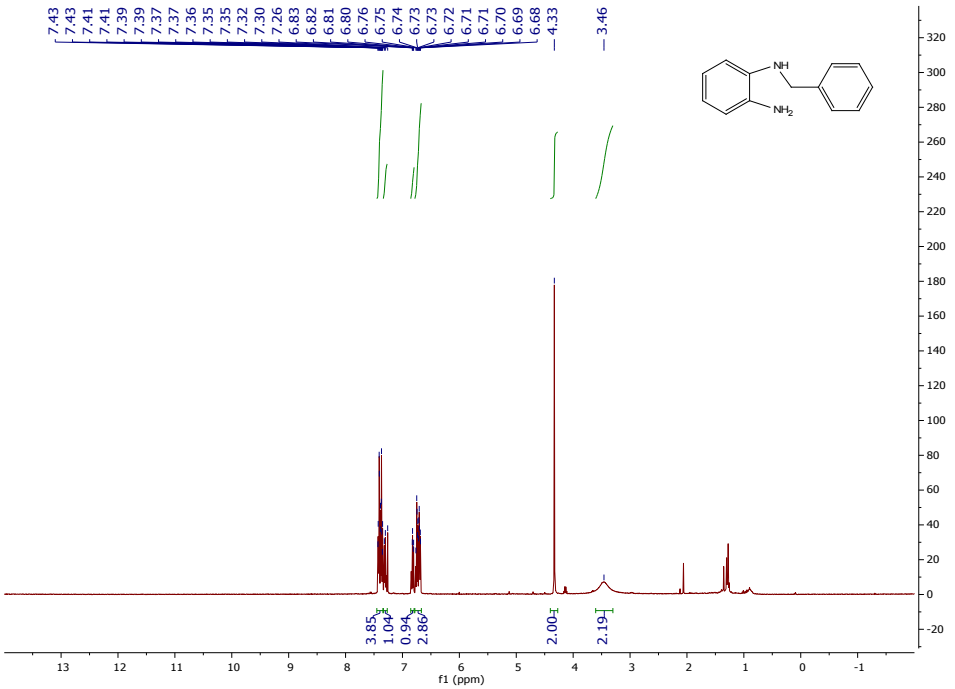

Figure S48. ^{1}H NMR (400 MHz, CD_3OD) of compound 18b.

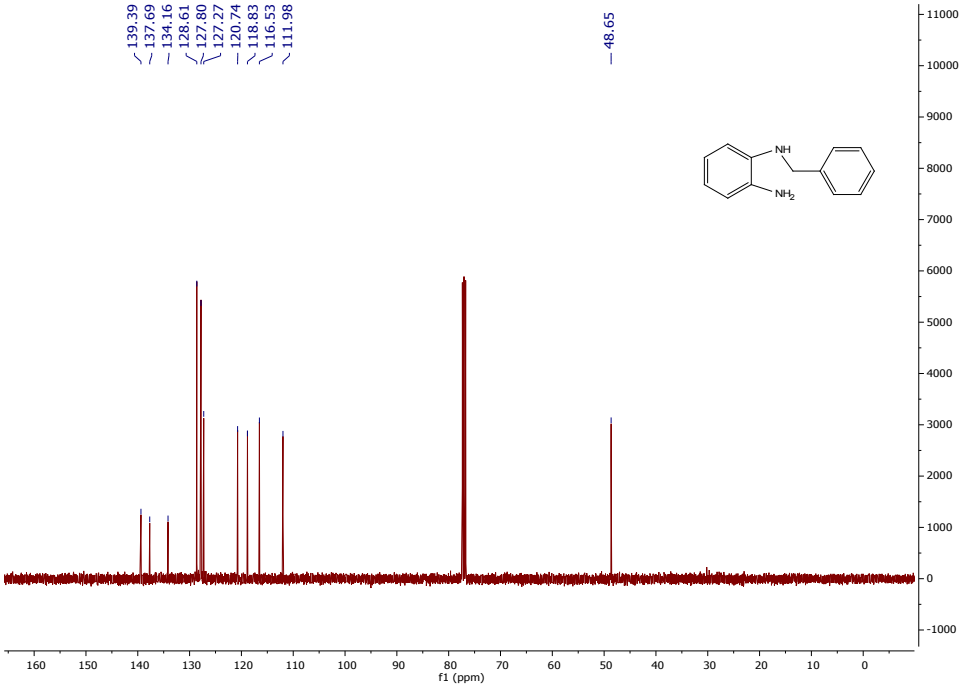

Figure S49. ^{13}C NMR (101 MHz, $CDCl_3$) of compound 18b.

References:

1 P. Kuzmic, *Anal. Biochem*., 1996, **237**, 260-273.

2 R. L. Manfro, T. P. M. D. Pires, N. F. P. Ribeiro and M. M. V. M. Souza, *Catal. Sci. Technol.*, 2013, **3**, 1278-1287.

3 J. Shen, J. M. Kobe, Y. Chen and J. A. Dumesic, *Langmuir*, 1994, **10**, 3902–3908.